National Library of Canada
Bibliothèque nationale du Canada

Canadian Theses Service
Service des thèses canadiennes

Ottawa, Canada
K1A 0N4

NOTICE

The quality of this microform is heavily dependent upon the quality of the original thesis submitted for microfilming. Every effort has been made to ensure the highest quality of reproduction possible.

If pages are missing, contact the university which granted the degree.

Some pages may have indistinct print especially if the original pages were typed with a poor typewriter ribbon or if the university sent us an inferior photocopy.

Reproduction in full or in part of this microform is governed by the Canadian Copyright Act, R.S.C. 1970, c. C-30, and subsequent amendments.

AVIS

La qualité de cette microforme dépend grandement de la qualité de la thèse soumise au microfilmage. Nous avons tout fait pour assurer une qualité supérieure de reproduction.

S'il manque des pages, veuillez communiquer avec l'université qui a conféré le grade.

La qualité d'impression de certaines pages peut laisser à désirer, surtout si les pages originales ont été dactylographiées à l'aide d'un ruban usé ou si l'université nous a fait parvenir une photocopie de qualité inférieure.

La reproduction, même partielle, de cette microforme est soumise à la Loi canadienne sur le droit d'auteur, SRC 1970, c. C-30, et ses amendements subséquents.

NL-339 (r. 88/04) c

Canada

Effect of Building Height on Dynamic Inelastic Response of Coupled Walls

By

Driss Chaker

A thesis
submitted in partial fulfillment of
the requirements for the degree of
Master of Applied Science

Department of Civil Engineering
Faculty of Engineering
University of Ottawa
Ottawa

© Driss Chaker, Ottawa, Canada, 1990

National Library of Canada
Bibliothèque nationale du Canada

Canadian Theses Service
Service des thèses canadiennes

Ottawa, Canada
K1A 0N4

The author has granted an irrevocable non-exclusive licence allowing the National Library of Canada to reproduce, loan, distribute or sell copies of his/her thesis by any means and in any form or format, making this thesis available to interested persons.

The author retains ownership of the copyright in his/her thesis. Neither the thesis nor substantial extracts from it may be printed or otherwise reproduced without his/her permission.

L'auteur a accordé une licence irrévocable et non exclusive permettant à la Bibliothèque nationale du Canada de reproduire, prêter, distribuer ou vendre des copies de sa thèse de quelque manière et sous quelque forme que ce soit pour mettre des exemplaires de cette thèse à la disposition des personnes intéressées.

L'auteur conserve la propriété du droit d'auteur qui protège sa thèse. Ni la thèse ni des extraits substantiels de celle-ci ne doivent être imprimés ou autrement reproduits sans son autorisation.

ISBN 0-315-60028-4

Canada

UNIVERSITÉ D'OTTAWA
UNIVERSITY OF OTTAWA

ABSTRACT

Coupled wall structures when subjected to earthquakes possess both strength and deformation capacity beyond the elastic range. Although coupled wall systems have a long history of satisfactory use in stiffening multistory buildings, there is a need for information on the behavior of such structures under strong earthquake motions.

Inelastic dynamic analysis was carried out in this research project to develop charts that show variation in ductility requirement with structure height when other strctural and ground motion parameters are kept constant. Three structures with different building height, and the same overall geometry were selected for analysis. A total of 20 coupled wall structures were analyzed in this investigation. Each structure was analyzed with different levels of yield strength and two different levels of beam-to-wall strength ratio.

The objective of the current study is to establish a relationship between height, strength and ductility requirement. An effort was made to express maximum wall and beam ductility requirement analytically for the coupled wall structures considered in this investigation.

ACKNOWLEDGEMENTS

The author wishes to express his sincere appreciation to his Supervisor, Dr. M. Saatcioglu for his advice, understanding and encouragement through this research project.

Thanks are due to my parents and my family for their understanding, patience and encouragement.

Acknowledgement is also extended to all my friends who gave me help and advice.

Contents

List of Figures

List of Tables

NOTATIONS

A	Cross Sectional area.
C	Damping Matrix.
C_1, C_2	Damping Constants.
E	Modulus Elasticity of Concrete.
EA	Axial Rigidity.
EI	Flexural Rigidity.
GA	Shear Rigidity.
h	Total Structure height.
I	Moment of inertia of a section.
I_e	Effective moment of inertia.
K	Stiffness.
L	Length of a member.
M	Bending moment.
M	Mass matrix.
M_Y	Yielding moment at flexural yield.
R	Beam-to-Wall strength ratio.
S	Elastic stiffness.
SI	Spectrum intensity of N-S Component of 1940 El Centro record.
T	Fundamental period of vibration.
T_1, T_2	Period for first and second modes, respectively.
t	Time increment.
V	Shear force.

ΔM	Increment of bending moment.
$\Delta M_A, \Delta M_B$	Increments of bending moment at member ends A and B, respectively.
ΔV	Increment of shear force.
$\Delta V_A, \Delta V_B$	Increments of shear force at member ends A and B, respectively.
K_s	Stiffness of a point hinge in elastic range ($= 1 \times 10^8$).
$\Delta r, \Delta \dot{r}, \Delta \ddot{r}$	Increments of displacement, velocity, and acceleration respectively.
ΔP	Increment load.
$\Delta\theta_A, \Delta\theta_B$	Increments of chord rotation at member ends A and B, respectively.
$\Delta\theta_A^e, \Delta\theta_B^e$	Increments of elastic chord rotation at member ends A and B, respectively.
$\Delta\theta_A^P, \Delta\theta_B^P$	Increments of plastic chord rotation at member ends A and B, respectively.
r	Reloading parameter for hysteretic loops.
$(\ )_W$	For Walls.
$(\ )_{BM}$	For Beams.
θ_{max}	Maximum rotation.
θ_Y	Rotation at yield.
μ_r	rotational ductility factor, ($\mu_r = \frac{\theta_{max}}{\theta_Y}$).

Chapter 1

Introduction

1.1 General

Seismic forces due to earthquakes occur in nature without any consistently recognizable warning. Lacking a suitable warning system, one must continue to rely heavily upon protective construction of buildings to reduce the adverse effects of earthquakes. Careful evaluation of earthquake damage that has occurred in reinforced concrete structures has led to many recent improvements in design procedures.

Reinforced concrete structural walls provide attractive means of seismic resistance because of their inherent strength and stiffness characteristics. Their stiffness also minimizes much of the non-structural damage during

a severe earthquake. Reinforced concrete walls in practice appear in the form of isolated walls, coupled walls or a wall-frame interactive system. Most shear walls contain vertical rows of openings for doors and windows. This produces two walls on either side of the openings, coupled by the members between the openings. The coupling of two or more walls by beams of moderate stiffness produces a substantial increase in stiffness of the resulting system as compared to uncoupled walls. The coupling action results in tensile and compressive axial forces in walls, and a reduction in bending moment in the individual walls.

Superiority of a coupled shear wall system in a seismic design can be explained by its ability to dissipate energy while maintaining substantial lateral stiffness. Under dynamic forces, most of the energy can be dissipated by significant yielding in beams while the walls continue providing overall stiffness and stability to the structure. Although coupled wall systems have a long history of satisfactory use in stiffening multistory buildings, not enough information is available on the behavior of such structures under earthquake motions. Knowledge on magnitudes of deformation and forces expected at critical regions of coupled wall systems under specific combinations of structural and ground motion parameters is essential for seismic design. Similarly, information on beam-to-wall strength and stiffness ratios is also required to control the sequence of plastification among members. Clarification of these aspects of coupled wall behavior can be accomplished through inelastic dynamic analysis. Once the proper analysis procedure is established, then the effects of structural and ground motion parameters

can be investigated. A design procedure can be developed using the design parameters.

Seismic effects on coupled wall structures were investigated by Saatcioglu et al. in the past (1,2,3). The previous investigation produced results on effects of structural and ground motion parameters. However, the results were, in most cases, limited to 20-story structures, for which the analysis results were generated. The effect of structure height on dynamic inelastic response of coupled walls has not been previously investigated. If a relationship is established between height of coupled walls, and structural parameters, this could lead to generalization of previous results. In this research program the effect of structure height on dynamic inelastic response of coupled wall structures is investigated.

1.2 Objective and Scope

The objective of the project is to establish relationships between structure height and dynamic response of coupled wall structures. It is intended to develop charts that show variation in ductility requirements with structure height when other structural and ground motion parameters are kept constant. The following outlines the scope:

1. Selection of coupled wall structures with different heights, while keeping some of the important structural parameters constant, for use in

dynamic analysis.

2. Identification of structural and ground motion parameters.

3. Dynamic inelastic analyses to investigate the effect of building height on inelastic response of coupled walls.

4. Development of design charts for coupled walls showing the variation of ductility requirements with building height.

1.3 Previous Research

In 1974 R.G.Oesterle et al.(4) at the Portland Cement Association, Skokie, Ill., conducted an investigation on behavior of reinforced concrete structural walls under load reversals. Sixteen large scale structural walls have been tested. These tests show that structural walls possess significant rotational ductility when subjected to reversing loads. The overall goal of the investigation was to develop design criteria to ensure adequate strength and ductility of structural walls and structural wall systems used in earthquake resistant construction.

The following conclusions were reported:

1. The observed hysteretic behavior and load deformation characteristics of structural walls are similar to those of beams.

2. Isolated structural walls possess significant inelastic deformation capacity when subjected to reversing loads. In general, the maximum rotational ductility decreases with increasing level of shear stress.

3. A significant increase in the amount of horizontal reinforcement has only a small effect on ductility prior to web crushing.

4. The observed relationship between "effective" shear distortions and flexural rotations may simplify the modeling of inelastic shear distortions.

In 1976, A.E.Fiorato et al.(5) carried out an experimental program to develop design criteria for reinforced concrete walls used as lateral bracing elements in earthquake resistant buildings. A combined experimental and analytical investigation of structural walls was carried out at the Portland Cement Association.

The objectives of the investigation were as follow :

1. To determine load versus deformation characteristics for a wide range of configuration of wall specimens.

2. To determine the ductility and energy dissipation capacity of walls subjected to reversing loads.

3. To determine the flexural and shear strengths of walls subjected to reversing loads, and to compare these strengths with the strength under monotonic loading.

4. To determine means of increasing the energy dissipation capacity of walls where required.

5. To develop design procedures for walls of adequate strength and energy dissipation capacity.

In this investigation, 5 walls were tested. Test results showed that either flexure or shear type failure was observed in the walls. These types were distinguished by the magnitude of the applied shear stress.

Vitelmo V. Bertero,(6) at the University of California Berkely, conducted experimental and analytical research on seismic behavior of isolated walls and coupling girders. The results indicate excellent hysteretic behavior, with adequate member ductility. Also, problems in designing coupled wall systems were examined. It was acknowledged that the use of coupled walls in seismic-resistant design have great potential. To realize this potential it would be necessary to prove that it is possible to design and construct "ductile coupling girders" and "ductile walls" that can supply the required strength, stiffness, and stability and dissipate significant amount of energy through stable hysteretic behavior of their critical regions.

In 1983, Saatcioglu et al.(2) conducted an analytical study on modeling hysteretic behavior of coupled walls for dynamic analysis. Emphasis was placed on effects of parameters defining the force-displacement hysteresis loops. Specifically, effect of axial force-moment interaction, strength reduction, shear yielding, pinching, reloading and unloading branches of hystere-

sis loops were considered. A 20 story coupled wall structure was selected for dynamic analysis. A modified version of computer program DRAIN-2D was used for the analysis. Each structural member was idealized as a line element. Program capabilities as modified by the Construction Technology Laboratories, included modeling of inelastic moment-rotation and shear-distortion relationships. Axial force-axial deformation relationships were considered to be linearly elastic through the investigation. Rotational ductility factor, defined as the ratio of maximum to yield rotations was used as a measure of inelastic deformation.

The main conclusions of the investigation are as follow:

1. Axial force-moment interaction effects due to coupling should be considered in dynamic analysis of coupled walls.

2. Rotational ductility requirements for coupling beams can be significantly increased by early and rapid strength reduction in hysteretic loops.

3. Variation in post yield loading, unloading and reloading branches of hysteretic loops within the range observed in tests, do not significantly affect dynamic response.

Saatcioglu et al.(1) in 1987 conducted a parametric investigation to determine the significance of selected structural and ground motion parameters on dynamic inelastic response of coupled wall structures. The structural parameters included :

stiffness and strength ratios, coupling arm, clear beam span, gravity loads, and structure mass. Ground motion parameters included: earthquake frequency characteristics, duration, and intensity. A computer program and a moment-rotation hysteretic model, including the effects of axial force-flexure interaction, was used to conduct nonlinear dynamic analyses. Over 50 analyses were carried out to identify the most significant parameters as design variables. The results provide guidance to structural engineers who are engaged in dynamic analysis of coupled wall structures for design purposes. The following conclusions were made:

1. Among the structural and ground motion parameters considered, the following can be classified as design parameters that deserve full attention during the design of an earthquake resistant coupled wall structure: fundamental period, wall strength, beam-to-wall stiffness ratio, beam-to-wall strength ratio, frequency characteristics of ground motion, and intensity of ground motion.

2. The degree of inelasticity in a structure is directly related to the flexural yield levels of members.

3. Beam-to-wall strength ratio is an important design parameter that controls the degree of coupling between the walls and the sequence of hinge development among members.

4. Maximum structural response increases almost linearly with the intensity of ground excitation. Therefore, results of analysis can be

extrapolated to predict structural response at different levels of earthquake intensities.

Chapter 2

Selection of Structures and Ground Motion for Dynamic Analysis

2.1 General

Use of coupled walls in practice was studied before selecting structures for dynamic inelastic analysis. Coupled walls are often used in multistorey buildings as stiffening members. Although structural walls are primarily used for lateral resistance to wind or earthquake forces, they are also used for functional reasons as permanent separators. Generally, isolated structural walls are coupled at floor levels by beams of moderate stiffness to

form coupled walls. Sometimes an isolated wall is pierced due to functional reasons such as window or door openings to form coupled walls. Use of coupled walls in buildings can be due to architectural and/or structural reasons.

Structural layout of buildings is influenced considerably by aesthetic and functional requirements. Office buildings generally require open office space with minimum interruption by vertical members. Therefore, central core exterior column or exterior wall interior column layouts have been generally favored . Structural walls in the form of elevator and stairway shafts can be effectively used to provide lateral stiffness to a multistorey building. For tall structures where more than one elevator shaft is used, it becomes necessary to provide corridor openings in walls. This leads to coupled walls. Similarly in the case of exterior walls, window openings may be necessary. Therefore, structural walls are usually pierced to form coupled walls. Fig 2.1 illustrates common use of coupled walls in office buildings.

Use of coupled walls is more common in residential buildings where walls can act as permanent partitions. Structural walls used in apartment, hotel, and other residential buildings provide acoustical privacy and fire separation. A more common use of coupled walls is to have them combined with gravity-load carrying frames. Fig 2.2 shows common use of coupled walls in apartment buildings.

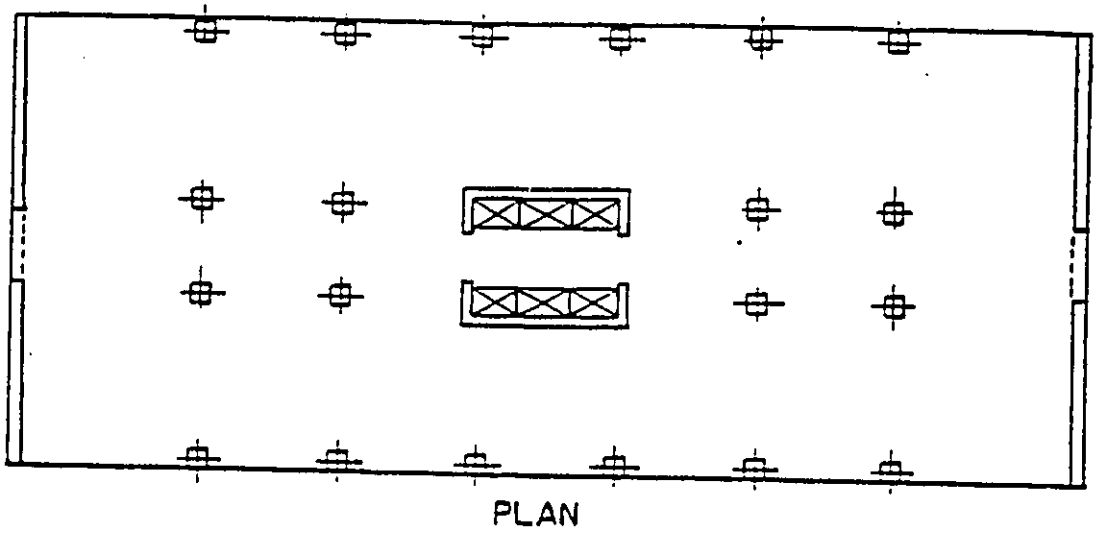

Figure 2.1: Common Use of Coupled Walls in Office Buildings

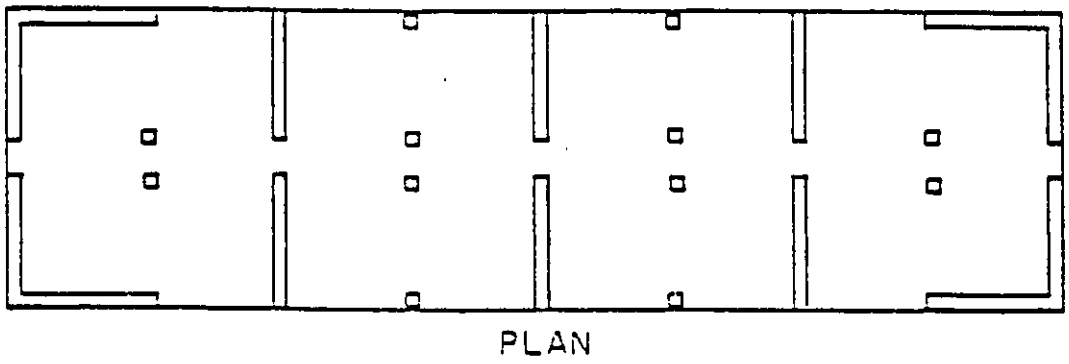

Figure 2.2: Common Use of Coupled Walls in Residential Buildings

2.2 Properties of Selected Structures

A 20-storey coupled wall structure was selected as a reference structure, to be used throughout the investigation. Structural and architectural functions, discussed in sec. 2.1 have been considered in selecting the reference structure. The structure floor plan was chosen to be symmetric in both directions as shown in Fig 2.3. Symmetry is generally desirable to minimize torsional effects, which are beyond the scope of this investigation.

Member properties of the structure were selected such that the fundamental period was 1.5 sec. Accordingly, the walls were 8 m wide and were coupled by beams having 3 m clear span length. Tributary masses were calculated for gravity and inertia forces separately since the columns were assumed to carry vertical loads only and walls were to resist earthquake induced inertia forces. Floor slabs were considered sufficiently stiff to cause all points on the same floor level to deflect by equal amounts horizontally. Since the objective of the current study is to investigate the effect of building height on dynamic structural response, two other structures, with essentially the same structural properties, but different building heights were also selected. These structures had 10-storey and 30-storey building heights. Fig 2.4 illustrates the elevation views of the three structures selected. Member geometry (and hence stiffness) was adjusted so that all three structures, i.e, 10-storey, 20-storey(reference) and 30-storey structures had the same fundamental period. Member sizes in each case were determined such that beam-to-wall stiffness ratio was the same in all three

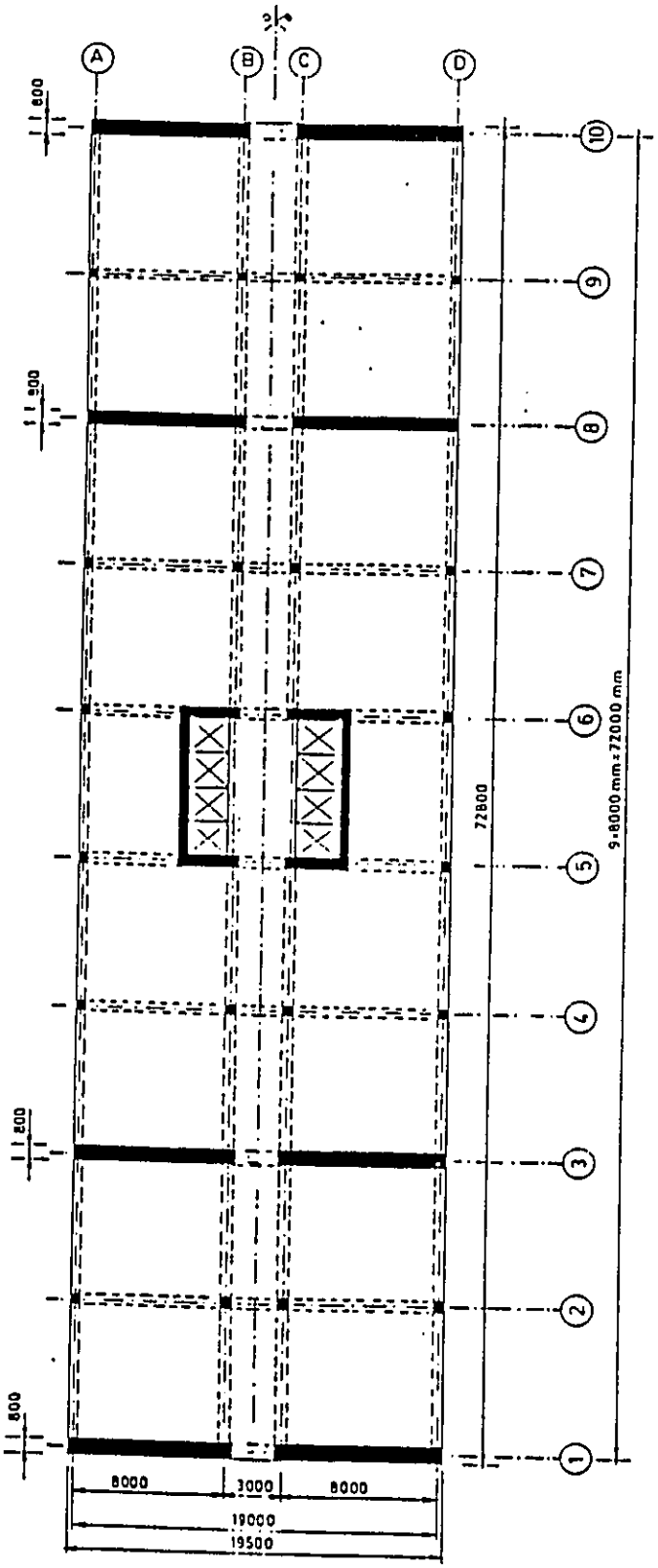

Figure 2.3: Structure Floor Plan Selected For Investigation

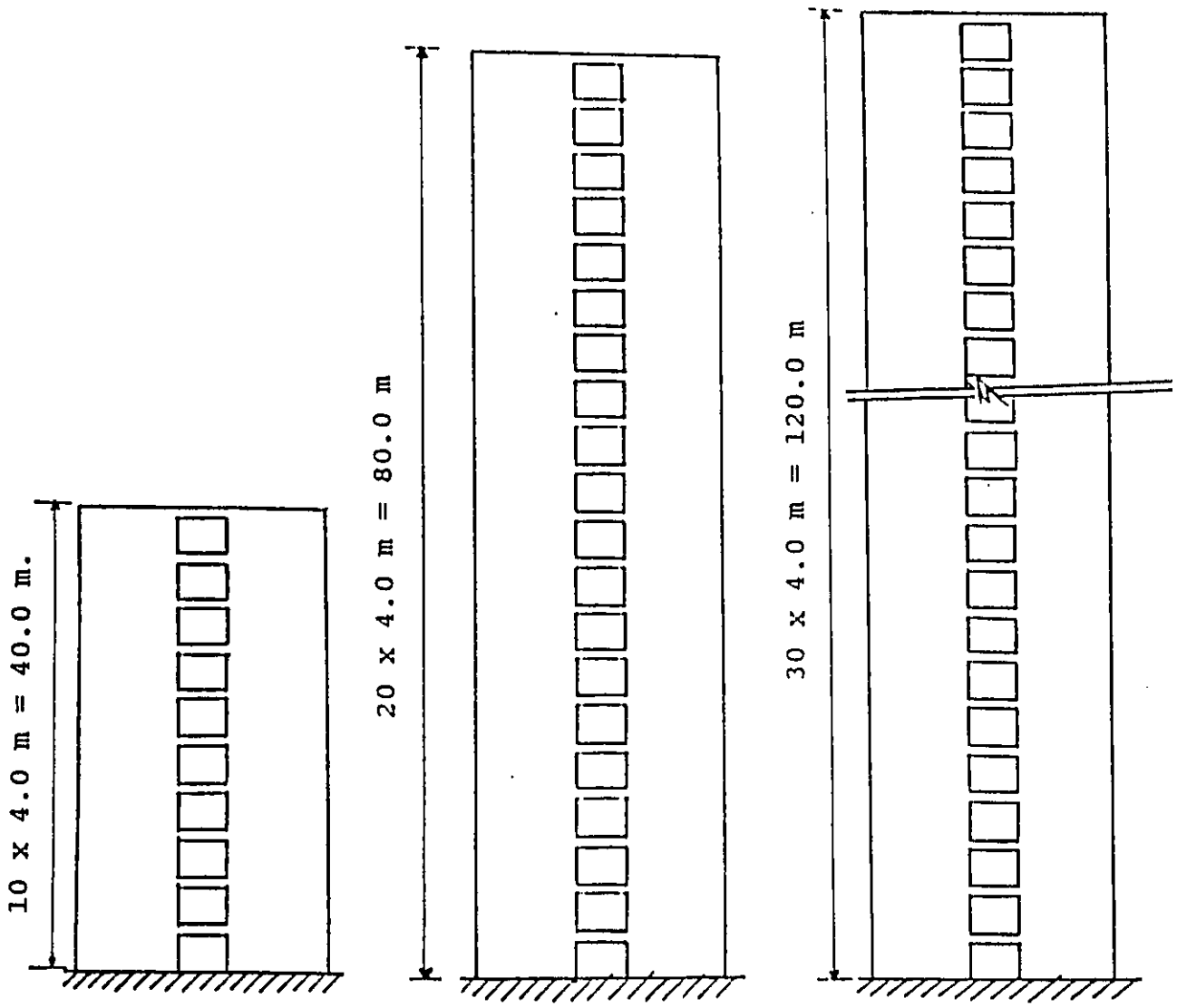

Figure 2.4: Structure Elevations

structures. This parameter, as well as the fundamental period were previously shown to have significant effects on structural response. Variation of structure height, while keeping other parameters constant would single out structure height as a parameter. However, to achieve the same fundamental period, the 10-storey structure member stiffnesses were reduced and the 30-storey structure member stiffnesses were increased. This resulted in unrealistic member sizes in these two structures. Table 2.1 provides a summary of member stiffnesses for the three structures selected.

Vibration periods of structures were determined using computer program DYFRQ. This program provided convenient means of solving the eigen value problem involved in determining the vibration periods.

2.3 Base accelerograms under consideration

For the dynamic analyses, six different accelerograms were selected to be considered as input ground motions. Fig 2.5 shows the 5%-damped response spectra for the first 10 sec of the accelerograms considered. In all cases intensity of each input motion was adjusted to yield a spectrum intensity equal to 1.5 times the spectrum intensity of the N-S component of the 1940 El-Centro record. Spectrum intensity here is defined as the area under the 5%-damped relative velocity response spectrum between periods of 0.1 and 3.0 seconds. 10 second duration of the normalized accelerograms considered are shown in Fig 2.6. Relative velocity response spectra for the input

motions considered are shown in Fig 2.5. The most critical input motion in terms of frequency content was selected from the response spectra. All the structures considered had a fundamental period of 1.5 sec. During response to earthquake motion the period of a structure is expected to elongate due to concrete cracking and steel yielding. It is estimated that the fundamental period of the structures considered will elongate beyond 2.0 sec during nonlinear response. Fig. 2.5 indicates that the 1940 El-Centro E-W record is critical for structures with a fundamental period of 2.0 sec or more. Therefore this earthquake record was selected for use in dynamic analyses.

All the structures analyzed were subjected to 10 sec of ground motion. Most strong-motion accelerograms contain high intensity oscillation during a 5 to 15 seconds phase. Studies of Bogdanoff (9) have shown that structures subjected to strong-motion accelerograms experience their peek relative displacements during this short intense phase. Other researchers, have also shown that damage to a structure is most likely to occur during the first 5 to 10 seconds of strong ground motion. Because of the need to limit the computer time required for analysis, the use of first 10 sec of ground motions was found adequate.

Table 2.1: Properties of Structures Selected for Parametric Investigation

Fundamental Period	1.5 Sec	1.5 Sec	1.5 Sec
Number of Stories	10	20	30
Wall height	40 m	80 m	120 m
Wall width	8 m	8 m	8 m
Clear beam span	3 m	3 m	3 m
Wall Stiffness Parameters			
EI	$0.555 * 10^8 kN.m^2$	$0.416 * 10^9 kN.m^2$	$2.662 * 10^9 kN.m^2$
GA	$0.350 * 10^7 kN$	$0.418 * 10^8 kN$	$0.167 * 10^9$ kN
EA	$0.822 * 10^7 kN$	$0.986 * 10^8 kN$	$0.394 * 10^9$ kN
Beam Stiffness parameters			
EI	$0.131 * 10^6 kN.m^2$	$0.981 * 10^6 kN.m^2$	$0.628 * 10^7 kN.m^2$
GA	$0.590 * 10^6$ kN	$0.702 * 10^7$ kN	$0.282 * 10^8$ kN
EA	$0.138 * 10^7$ kN	$1.658 * 10^7$ kN	$0.664 * 10^8$ kN
Wall Yield Moment,M_Y	20,000 kN.m	70,000 kN.m	120.000 kN.m
Beam Yield Moment	300 kN.m	1050 kN.m	1800 kN.m
Weight	780 kN/Wall	1000 kN/Wall	3741 kN/wall
Weight for Inertia Forces	3158 kN	3109 kN	8364 kN
Base Fixity Condition	Fully fixed	Fully fixed	Fully fixed
Ground Motion	El-centro 1940 E-W	El-centro 1940 E-W	El-centro 1940 E-W

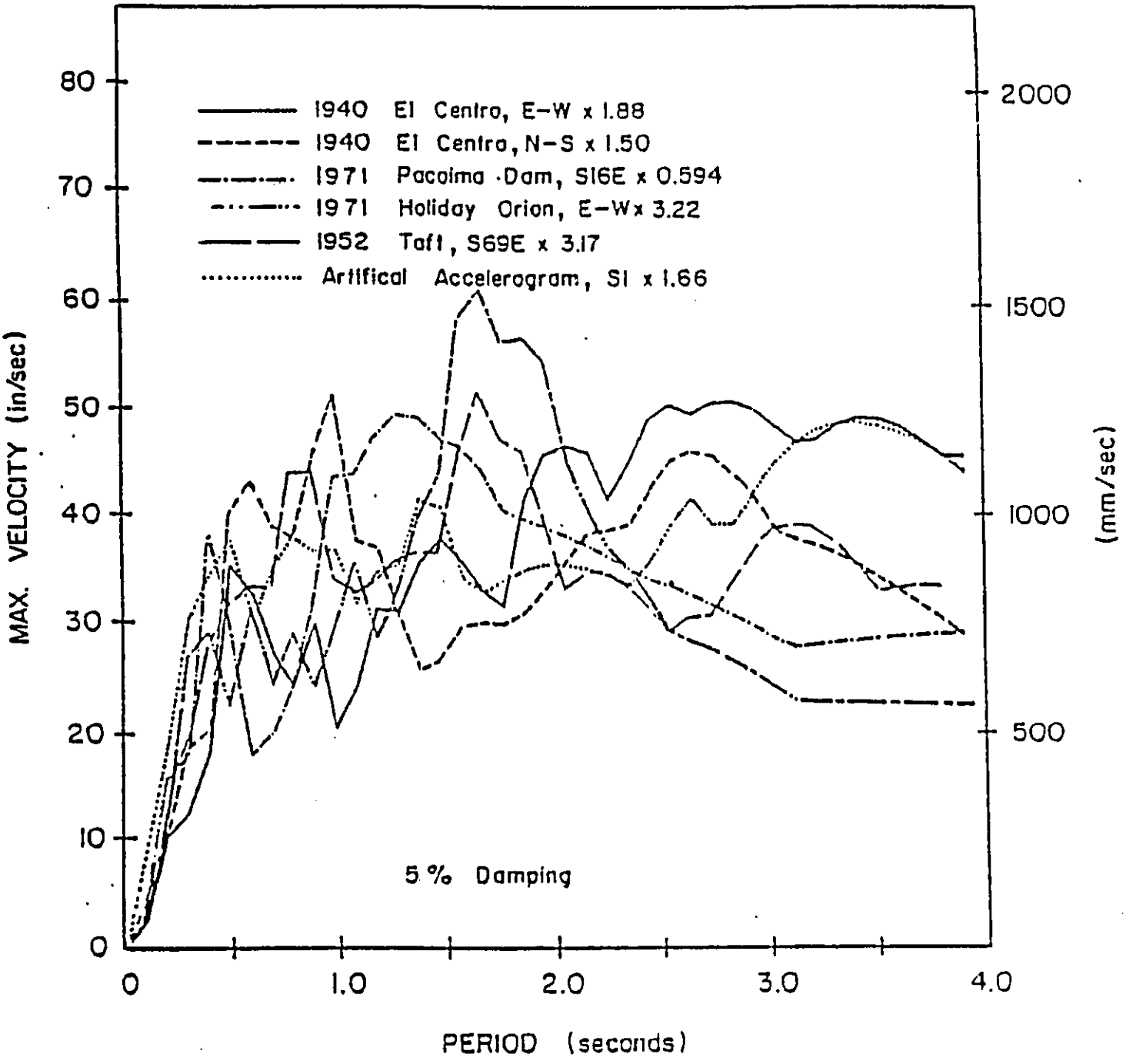

Figure 2.5: Relative Velocity Response Spectra for First Ten-Seconds of Normalized Input Motions

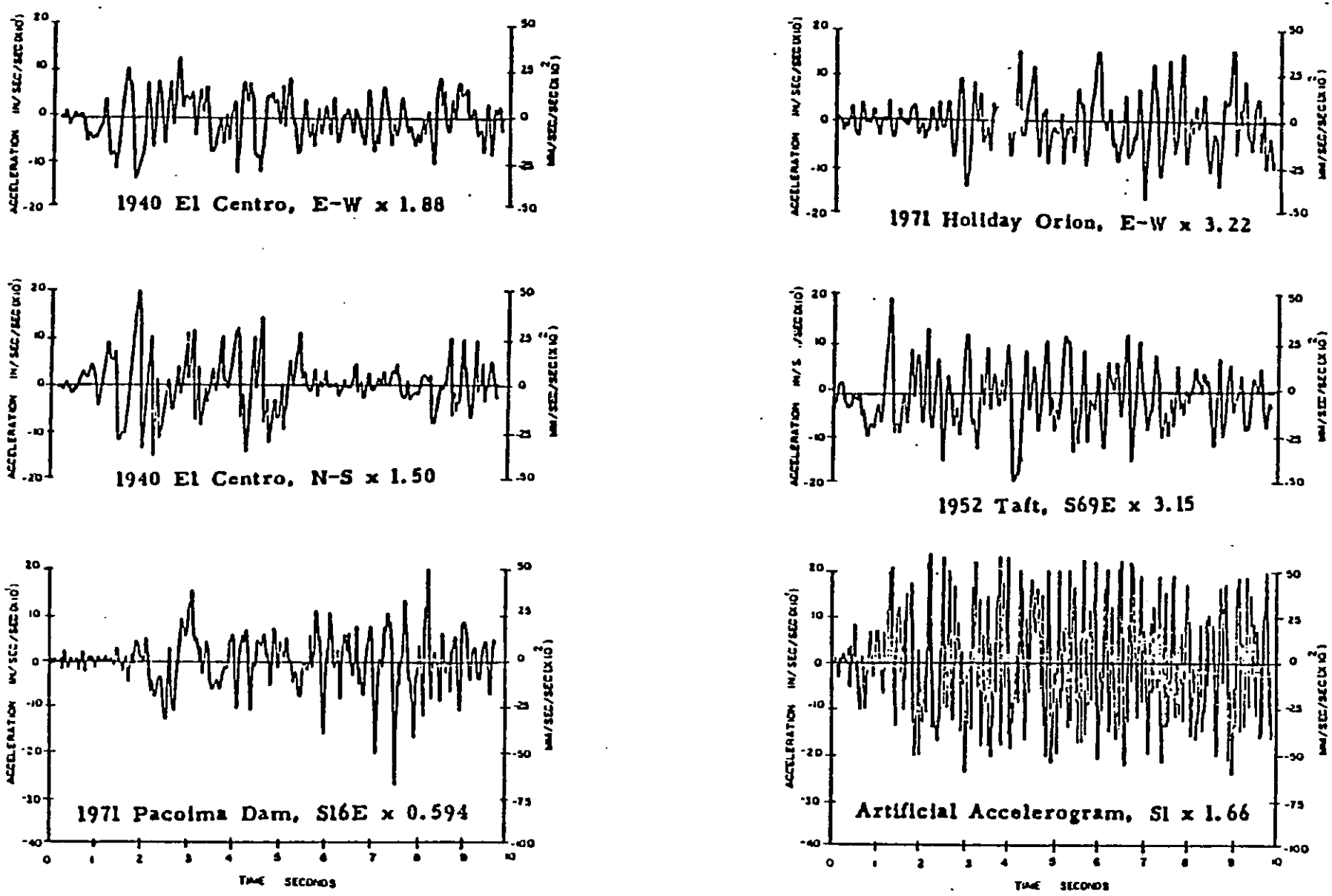

Figure 2.6: Ten-Second Duration Normalized Accelerograms

Chapter 3

Procedure for Dynamic Analysis

It is generally agreed that under strong earthquakes inelastic behavior of structures is inevitable. Therefore dynamic analysis of structures under earthquake excitations should properly consider inelastic action. In this investigation, dynamic inelastic response analysis was employed. A computer program was used to investigate nonlinear response of coupled wall structures. Description of the computer program and the modeling procedures used are discussed in the followings sections.

3.1 Computer program DRAIN-2D

Dynamic response analysis was carried out using the program DRAIN-2D developed at the University of California at Berkeley by A.E.Kanaan ,and G.H.Powell in 1972. It was modified by the Portland Cement Association, Illinois in 1979. The program was later implemented to the University of Ottawa AMDAHL computer. The program has the capabilities to analyze plane inelastic structures under seismic excitation. The structural stiffness matrix is formulated by the direct stiffness method, with nodal displacements as unknowns. Each element in a structure is idealized as a planar discrete element. Each element has two nodes, one at each end, and each node possesses three degrees of freedom. Since the program is limited to plane structures, degrees of freedom at each node are translations in x, and y directions, and rotation about z axis. The element stiffness matrix is formulated for each element. The structure stiffness matrix is assembled from the element stiffness matrices.

Dynamic response is determined using step-by-step integration assuming a constant response acceleration during each time step. At any time step an equation of dynamic equilibrium can be written as :

$$[M]\{\Delta\ddot{r}\} + [C]\{\Delta\dot{r}\} + [K]\{\Delta r\} = \{\Delta p\} \tag{3.1}$$

where: $\{\Delta\ddot{r}\}, \{\Delta\dot{r}\}, \{\Delta r\} and \{\Delta p\}$ are finite increments of acceleration, velocity, displacement, and load respectively.$[M], [C], [K]$ are the mass, damping and stiffness matrices respectively.

The structure mass is assumed to be lumped at the nodes. This leads to a diagonal mass matrix. Viscous damping is assumed resulting from a combination of mass dependent and stiffness dependent effects. The damping matrix can be written as :

$$[C] = C_1[M] + C_2[K] \tag{3.2}$$

Where; C1 and C2 are constants, and are based on the first and second mode effects.

$$C_1 = \frac{4\pi(T_1\lambda_1 - T_2\lambda_2)}{{T_1}^2 - {T_2}^2} \tag{3.3}$$

$$C_2 = \frac{T_1T_2(T_1\lambda_1 - T_2\lambda_2)}{{T_1}^2 - {T_2}^2} \tag{3.4}$$

In which T_1, T_2 and λ_1, λ_2 are the periods and percentages of critical damping for the first and second modes respectively.

The program contains different types of elements for different use . The element that is of interest in this investigation is the beam element.

3.2 Element Idealization for Computer Analysis

In computer program DRAIN-2D each wall and beam element between joints is idealized by a line element. It is extremely important to specify properties of these line elements properly so that both elastic and inelastic

behavior of individual members can be simulated accurately. While the load deformation relationship for the elastic region is straightforward, representation of hinging region of walls and beams requires special attention. Inelastic action is introduced by allowing the formation of plastic hinges at the end of line elements. Thus, each element consists of an "elastic beam" and "two potential point hinges", one at each end, as shown in Fig. 3.1. Since the computer model and the actual structure should yield the same behavior, stiffnesses of elastic beam and point hinges should be specified such that total chord rotation of a line in the model is equal to chord rotation of the actual member. If a member is in the elastic range then the point hinges are assigned infinitely large stiffnesses and hence do not rotate. In this range the elastic beam is assigned the elastic stiffness of the member and deforms accordingly. If the force level exceeds the prescribed yield level, then the point hinges at member ends become active and start rotating to simulate yielding.

3.3 Modeling for Flexure

If moment-rotation characteristics of a member are known, then the flexural properties of the elastic beam and the point hinges can be determined. Primary moment-rotation relationship of a reinforced concrete member can be simplified as a bilinear relationship. This means that the primary curve of a typical member consists of two linear segments, one representing the elastic range and the other the post yield of inelastic range . Fig. 3.2 shows

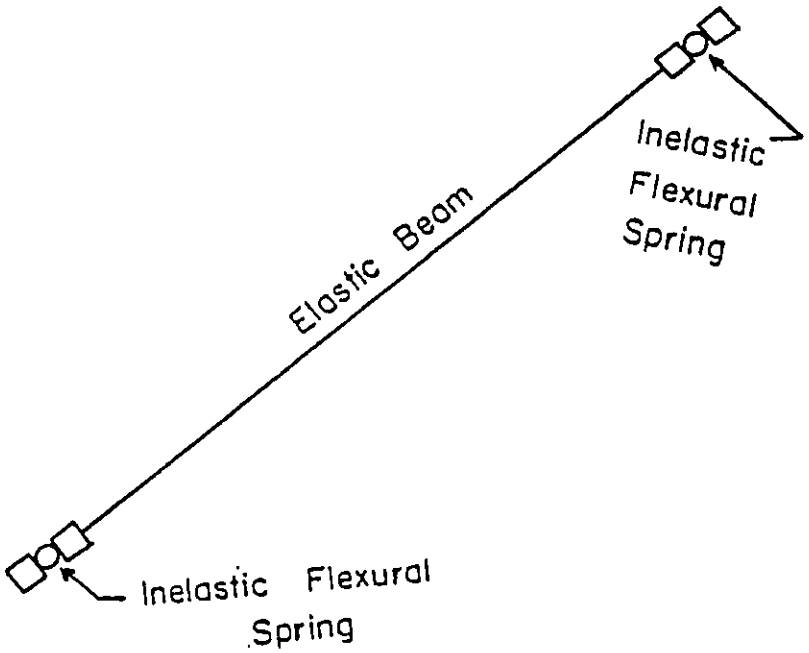

Figure 3.1: Element Idealization

representation of moment-rotation diagram of a wall element in terms of moment rotation diagrams of its idealized components, i.e., the elastic beam element and the point hinges.

Chord rotation of a member is calculated as the sum of elastic beam rotation and plastic hinge rotations. Thus,

$$\Delta\theta_A = \Delta\theta_A^e + \Delta\theta_A^p \tag{3.5}$$

$$\Delta\theta_B = \Delta\theta_B^e + \Delta\theta_B^p \tag{3.6}$$

$\Delta\theta_A^e, \Delta\theta_B^e$ are increments of chord rotations due to bending of the elastic beam. $\Delta\theta_A^p, \Delta\theta_B^p$ are increments of rotations of the point hinges at the ends "A" and "B" respectively. For an element AB, incremental moment-rotation relationships for elastic and plastic components can be written as shown below.

$$\begin{Bmatrix} \Delta\theta_A{}^e \\ \Delta\theta_B{}^e \end{Bmatrix} = \begin{bmatrix} \frac{L}{3EI} & -\frac{L}{6EI} \\ -\frac{L}{6EI} & \frac{L}{3EI} \end{bmatrix} \begin{Bmatrix} \Delta M_A \\ \Delta M_B \end{Bmatrix} \tag{3.7}$$

$$\begin{Bmatrix} \Delta\theta_A{}^p \\ \Delta\theta_B{}^p \end{Bmatrix} = \begin{bmatrix} \frac{1}{\alpha_A K_s} & 0 \\ 0 & \frac{1}{\alpha_B K_s} \end{bmatrix} \begin{Bmatrix} \Delta M_A \\ \Delta M_B \end{Bmatrix} \tag{3.8}$$

The quantity K_s is specified as having a very large value within the elastic range, implying that the point hinges do not rotate prior to yielding. This leaves only the elastic beam component to rotate to simulate the behavior of an actual concrete member in the elastic range. Then the increments of total flexural chord rotations can be written from equation (3.7).

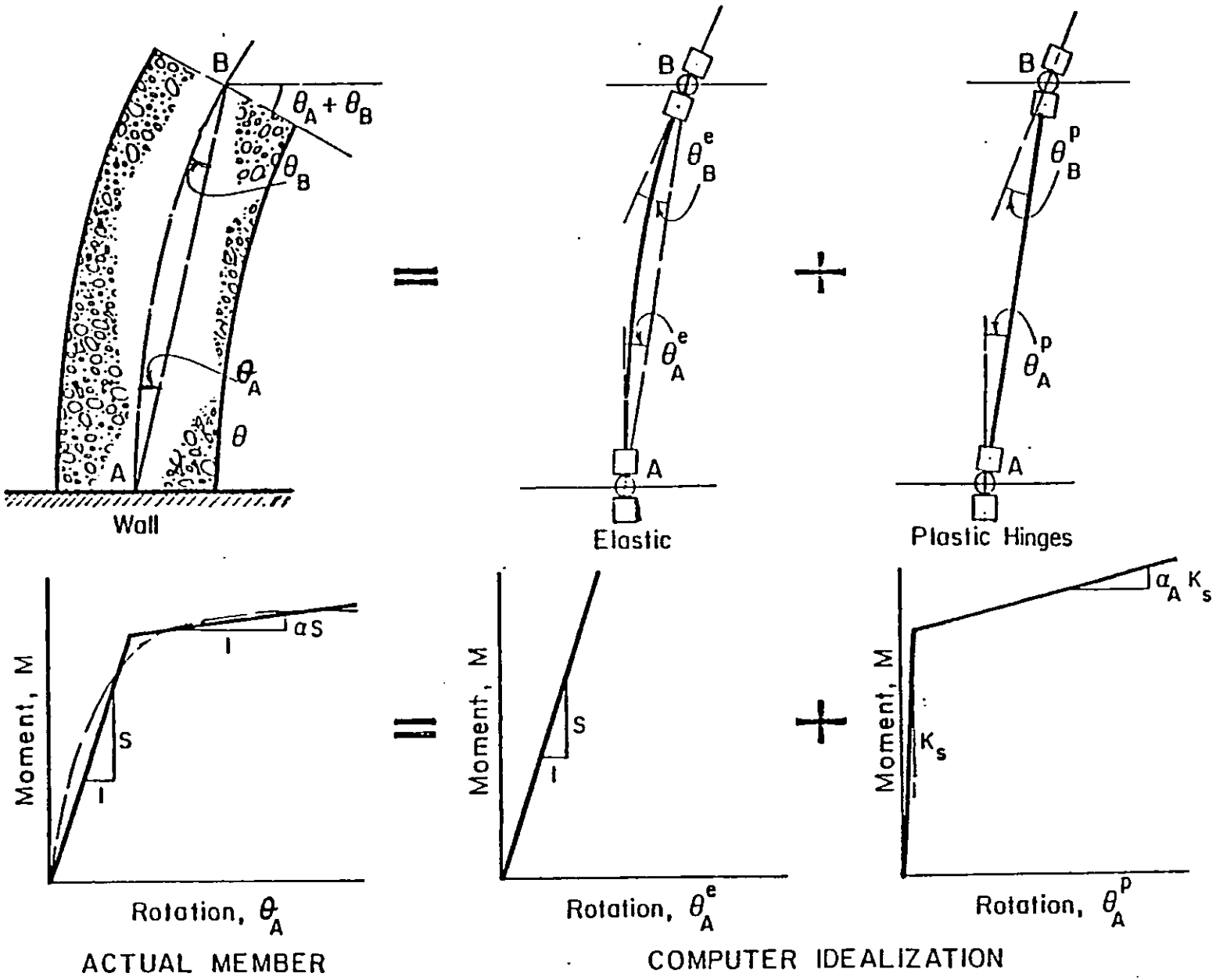

Figure 3.2: Modelling Wall Element

$$\Delta\theta_A = \Delta\theta_A^e = \frac{L}{3EI}\Delta M_A - \frac{L}{6EI}\Delta M_B \tag{3.9}$$

$$\Delta\theta_B = \Delta\theta_B^e = -\frac{L}{6EI}\Delta M_A + \frac{L}{3EI}\Delta M_B \tag{3.10}$$

Equations (3.9) and (3.10) indicate that it is sufficient to specify the effective stiffness parameter (EI) to establish the moment-rotation relationship in the elastic range .

If the moment level exceeds the prescribed yield level, then the point hinges at member ends become active and start rotating to simulate yielding. Within the inelastic range, chord rotation at one end is equal to the sum of elastic beam rotation and plastic hinge rotation at that end. Total incremental flexural rotations at member ends can be written by adding equations (3.7) and (3.8).

$$\Delta\theta_A = \frac{L}{3EI}\Delta M_A - \frac{L}{6EI}\Delta M_B + \frac{1}{\alpha_A K_s}\Delta M_A \tag{3.11}$$

$$\Delta\theta_B = -\frac{L}{6EI}\Delta M_A + \frac{L}{3EI}\Delta M_B + \frac{1}{\alpha_B K_s}\Delta M_B \tag{3.12}$$

α_A, α_B are ratios of the slope of the post yield branch to the slope of the elastic branch of the bilinear moment-rotation curves characterizing the point hinges at member ends "A" and "B", respectively. These two ratios can be determined by imposing the condition that total chord rotation of the model be equal to chord rotation in the real member.

Increments of flexural chord rotation of a real member beyond yielding can be written as :

$$\Delta\theta_A = \frac{L}{3\alpha EI}\Delta M_A - \frac{L}{6\alpha EI}\Delta M_B \tag{3.13}$$

$$\Delta\theta_B = \frac{L}{6\alpha EI}\Delta M_A - \frac{L}{3\alpha EI}\Delta M_B \tag{3.14}$$

Where "αEI" is the effective stiffness parameter of the member beyond yielding. This effective stiffness represents a uniform member stiffness and corresponds to the slope of inelastic branch of the bilinear member rotation idealization, as shown in Fig 3.2. In the same idealization,"α" denotes the ratio of inelastic stiffness to elastic stiffness.

Equating $\Delta\theta_A$ and $\Delta\theta_B$ from equations (3.11) and (3.12) which where developed for the computer model, to corresponding values from equations (3.13) and (3.14) which where developed for the real member, yields expressions for "α_A" and "α_B"

$$\alpha_A = \frac{3EI}{L}\frac{\alpha}{(1-\frac{\xi}{2})}\frac{1}{(1-\alpha)}\frac{1}{K_s} \tag{3.15}$$

$$\alpha_B = \frac{3EI}{L}\frac{\alpha}{(1-\frac{1}{2\xi})}\frac{1}{(1-\alpha)}\frac{1}{K_s} \tag{3.16}$$

where;

$$\xi = \frac{M_B}{M_A} \tag{3.17}$$

The above equations can be used to determine stiffness ratios of point hinges in the computer model if the bilinear moment chord-rotation relationship of the real member is known.

3.4 Modeling Wall Elements

Variation of moment along the height of structural walls is generally gradual and can be regarded as almost uniform between any two floors. Fig. 3.3 shows a moment diagram of a wall element at the base. Since the moment in an element can be considered uniform, the sectional moment-curvature relationship has the same shape as the moment chord rotation relationship. For walls of the coupled wall structure considered in this investigation the ratio of inelastic to elastic slopes of bilinear moment-curvature relationship α was taken as 0.05 . In solving equations (3.15) and (3.16) "ξ" can be taken as approximately -0.8. It should be noted that according to the sign convention used in deriving the expressions for chord rotations, clockwise moments at member ends are positive. Therefore the ratio of moments at the ends of a wall element, bent in single curvature, has a negative sign.

The stiffness parameter of point hinges in the elastic range is "K_s". This parameter is assigned a very large value to prevent rotation of point hinges during elastic action . A value of $K_s = EI * 10E8$ is used for modeling wall elements.

3.5 Modeling Beam Elements

Coupling beams behave differently than wall elements. The main difference is the double curvature configuration that occurs in beams when the

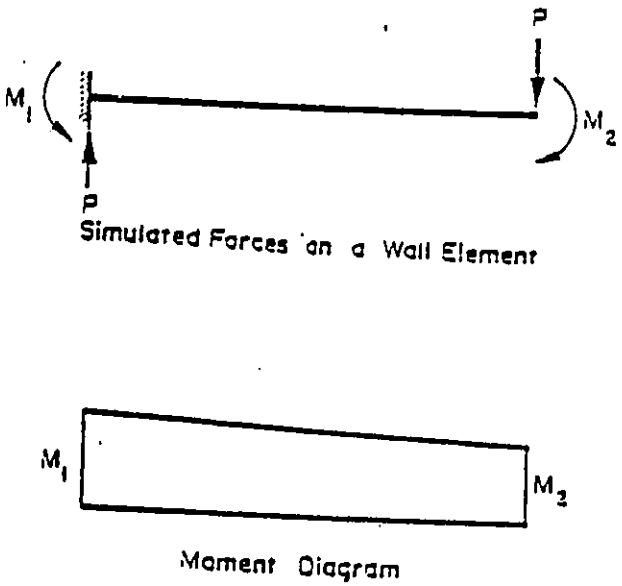

Figure 3.3: Moment Diagram of Wall Element at the Base

structure displaces laterally under earthquake-induced inertia forces. This implies that in the absence of gravity loads, the moment for coupling beams shows a linear variation with opposite signs at each end. Consequently, formation of hinges may take place at two ends . These hinges rotate in opposite directions. For a symmetric wall system with symmetrically reinforced coupling beams, it is reasonable to assume a symmetric moment distribution . Fig. 3.4 shows variation of moment and formation of point hinges in a coupling beam element. To determine properties of the point hinges at member ends, it is necessary to establish a bilinear idealization of the moment-chord rotation relationship.

For beams of the coupled wall structure selected for this investigation the ratio of inelastic to elastic slopes of bilinear moment-chord rotation rela-

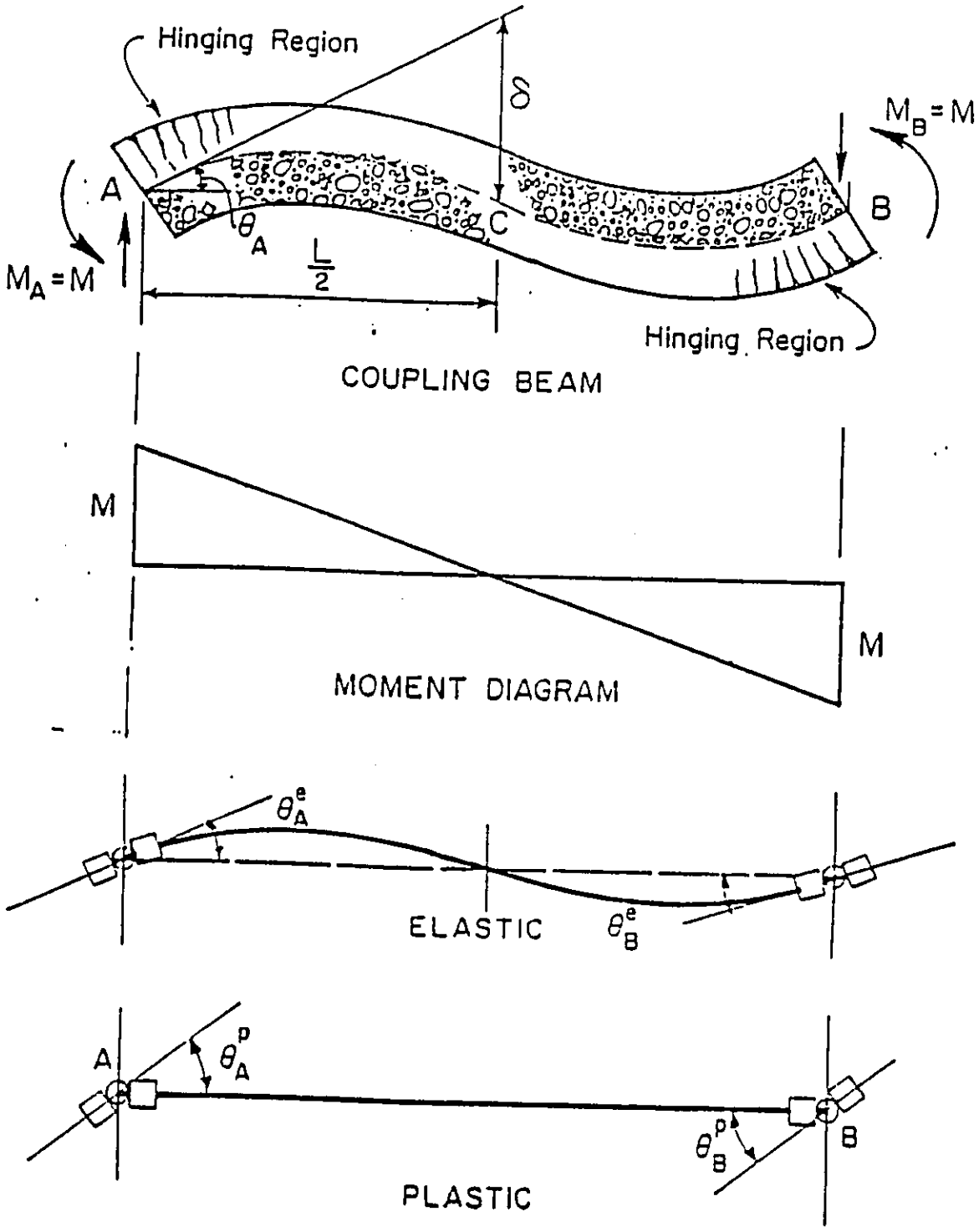

Figure 3.4: Modeling Beam Members

tionship "α" was taken as 0.06. In solving equations (3.15) and (3.16),the moment ratio "ξ" was taken as 1.0 due to symmetry in the moment diagram

.

3.6 Modeling for Shear

Modeling for shear is done in much the same manner as for flexure. If the shear force-shear distortion relationship of a member is known, then characteristics of the primary shear-shear distortion curve for the analytical model can be determined. In this investigation elastic shear behavior was assumed. The effect of shear cracking and softening in shear rigidity is considered by empirically reducing the elastic shear rigidity GA. The following shear-versus-shear distortion relationship can be written for the elastic component in an element AB.

$$\begin{bmatrix} \Delta\gamma_A^e \\ \Delta\gamma_B^e \end{bmatrix} = \begin{bmatrix} \frac{1}{GA} & 0 \\ 0 & \frac{1}{GA} \end{bmatrix} \begin{bmatrix} \Delta V_A \\ \Delta V_B \end{bmatrix} \tag{3.18}$$

where;

$\Delta\gamma_A^e$ *and* $\Delta\gamma_B^e$ are increments of chord angle rotations due to elastic shear distortions in the elastic beam at member ends " A" and "B" respectively.

Moments and shears in a member are directly related to each other through equilibrium equations. In Drain-2D, flexural and shear stiffnesses are combined as follows.

$$\begin{bmatrix} \Delta\theta_A \\ \Delta\theta_B \end{bmatrix} = \begin{bmatrix} \frac{L}{3EI} + \frac{1}{\alpha_A K_s} + \frac{1}{LGA} & -\frac{L}{6EI} + \frac{1}{LGA} \\ -\frac{L}{6EI} + \frac{1}{LGA} & \frac{L}{3EI} + \frac{1}{\alpha_B K_s} + \frac{1}{LGA} \end{bmatrix} \begin{bmatrix} \Delta M_A \\ \Delta M_B \end{bmatrix} \quad (3.19)$$

In this equation, $\Delta\theta_A$ and $\Delta\theta_B$ are total incremental chord angles at element ends "A" and "B" respectively, i.e., including elastic and plastic flexural and elastic shear deformations. The modeling procedure discussed above is used to establish the primary force-deformation relationship.

3.7 Bilinear Idealization of Primary Curve

A number of assumptions are made in modeling nonlinear behavior of members. Most of these assumptions are related to idealization and modeling of nonlinear force-deformation relationships.

Moment-rotation relationships of members are idealized as bilinear curves. Fig. 3.5 illustrates a typical primary moment-rotation relationship for reinforced concrete members and its idealization as two line segments. The first line segment represents effective stiffness in the elastic range, and the second line segment represents post yield stiffness. Depending on specifics of a given moment-rotation relationship, a number of rules may be devised to select slopes of these line segments and corresponding magnitude of yield moment. Member section details, especially locations of reinforcing bars, may have a significant effect on the general character of moment-rotation

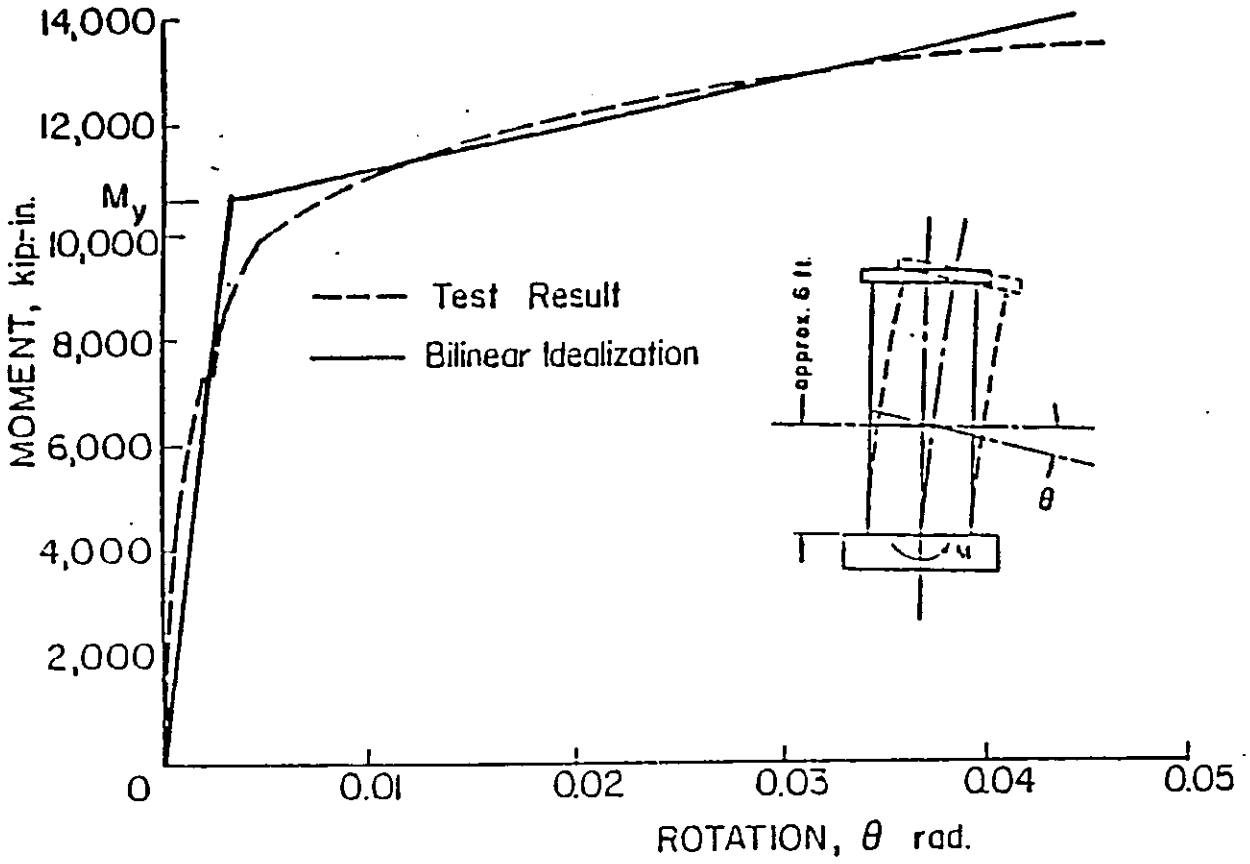

Figure 3.5: Bilinear Idealization of Moment-Rotation Relationship

relationship. Thus, members with the bulk of flexural reinforcement concentrated near the ends of the section exhibit a relatively well defined break (yield point) in their moment rotation relationship. Some members, on the other hand, show progressive yielding and do not exhibit a clear yield point. In arriving at a bilinear idealization of a particular force-displacement relationship, a number of approaches can be used. The simplest and most obvious would be a visual "sketched-in" approximation to the given curve. However, more specific quantitative criteria are desirable in the interest of reproducibility. Such rules can then be applied uniformly to any number of widely varying cases. For instance best fit lines in the least squares sense could be obtained for specific ranges of deformation.

A more commonly used method applies the criterion of equal area under the actual and idealized curves over a reasonable range of deformation. In this case the intersection of effective elastic and post-yield line segments defines the yield point. The actual force-displacement curve will include effects of cracking as well as any softening due to bond slip.

The ratio of inelastic to elastic slopes of idealized moment chord rotation relationship will vary with individual member properties. However, this variation is usually small and therefore is not expected to have any significant effect on dynamic response. Variation in the inelastic slopes of coupling beams and walls were shown to have little effect on dynamic inelastic response.

3.8 Characteristics of Hysteretic Loops

In the analytical model, inelasticity is introduced through point hinges at member ends. Therefore, behavior of members under inelastic load cycles is simulated by assigning load deformation hysteretic loops to the point hinges.

Reinforced concrete members generally exhibit degrading stiffness properties when subjected to load cycles. Degradation in stiffness occurs during unloading and reloading. This behavior was modeled by Takeda and was adopted here with some minor changes. General behavior of Takeda's model is shown in Fig 3.6. The primary curve of the model is bilinear, with initial elastic stiffness and a subsequent post yield stiffness, which are monotonic loading characteristics. When the reversed load is applied, stiffness degradation is introduced. The unloading stiffness is assigned a value which is less than the initial elastic stiffness. Reloading slope of hysteretic loop (stiffness) is determined by assuming loading towards the previous maximum deformation. This implies that as the level of maximum deformation increases, the magnitude of reloading stiffness decreases. Modifications introduced to Takeda's model which were implemented into program DRAIN-2D, include parameters "u" and "r" to control unloading and reloading slopes. Fig 3.7 illustrates the meaning of these parameters.

The original Takeda's model was developed for members under constant axial force. However, coupled walls generally undergo substantial changes

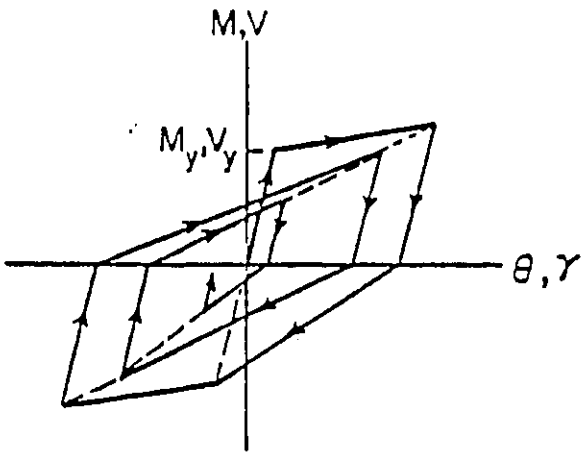

Figure 3.6: Takeda's Hysteretic Loop

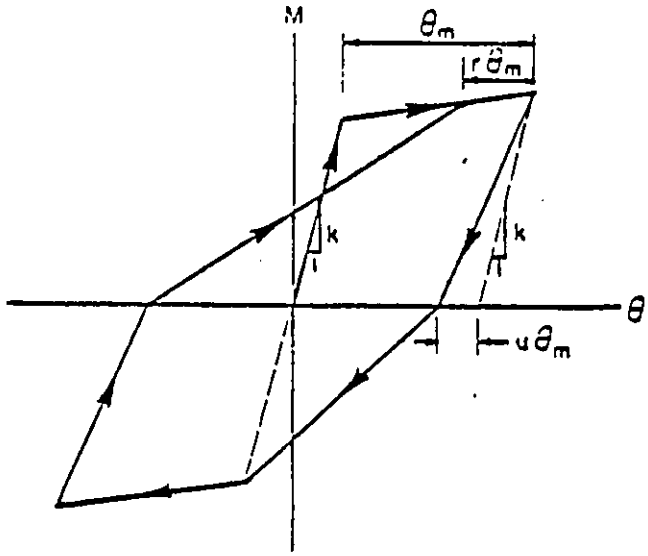

Figure 3.7: Unloading and Reloading Parameters of Hysteretic Loop

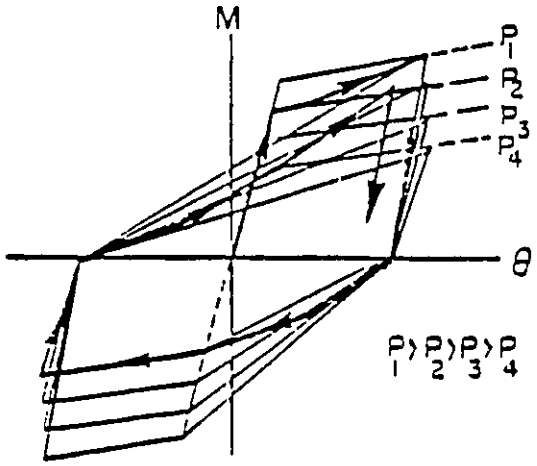

Figure 3.8: Hysteretic Loop Under Changing Axial Forces

in the level of axial force during response to earthquake motions. Because of this continuous change in axial force and the interaction between axial force and bending moment, the yield moment changes continuously. This interaction not only alters the initial yield level, but also affects the effective stiffness of the structure in the post-yield range. Therefore, the basic degrading stiffness model was modified by Saatcioglu et al.(2) to include axial force-flexure interaction. The modified model is shown in Fig. 3.8. It was implemented into program DRAIN 2-D and was used in this investigation.

3.9 Rotational Ductility Factor

The general concept of inelastic design against earthquake forces is well accepted in current design practice. The aim in inelastic design is to design critical regions of structures so that the required inelastic action can take place without significant loss of strength or excessive deformation. A measure of this inelastic action is difficult to define if it's to cover all aspects of inelastic deformation capacity.

A commonly accepted measure of inelastic deformation is the ductility factor or ratio. In this investigation, the rotational ductility factor is used as a measure of inelastic action, and defined as :

$$\mu_r = \frac{\theta_{max}}{\theta_y} \tag{3.20}$$

where;

θ_{max} is the maximum rotation and θ_y is the yield rotation. Usually rotations referred to here are the rotations of the hinging region. Generally, width of walls is equal to or greater than floor-to-floor height. If we assume the hinging region to have a height approximately equal to the wall width , then an entire wall element between floors in the model structure would form part of the hinging region. For this case, it would be appropriate to speak of ductility associated with the entire element. In terms of rotational deformation, the total rotation in the element would be given by the sum of chord rotations at both ends of an element. This total rotation in an element is made up of the sum of point hinge rotations and elastic chord rotations at both ends as shown in Fig. 3.3. Yield rotation is taken as the sum of elastic chord rotations at both ends when the moment in the member is equal to the yield moment.

The same basic definition of Ductility is used for coupling beams. However, because coupling beams are generally bent in double curvature, as compared to single curvature prevalent in walls, a slightly different method is used in calculating ductility. In a coupling beam bent in an antisymmetrical mode, hinges can form at each end but rotate in opposite directions. Because of this, hinges in coupling beams are generally limited in extent to one-half the span. In this case, ductility at one end is based on chord rotation at that end rather than the sum of the chord rotations at both ends used for walls.

Further clarification of the definition of the ductility for coupled wall

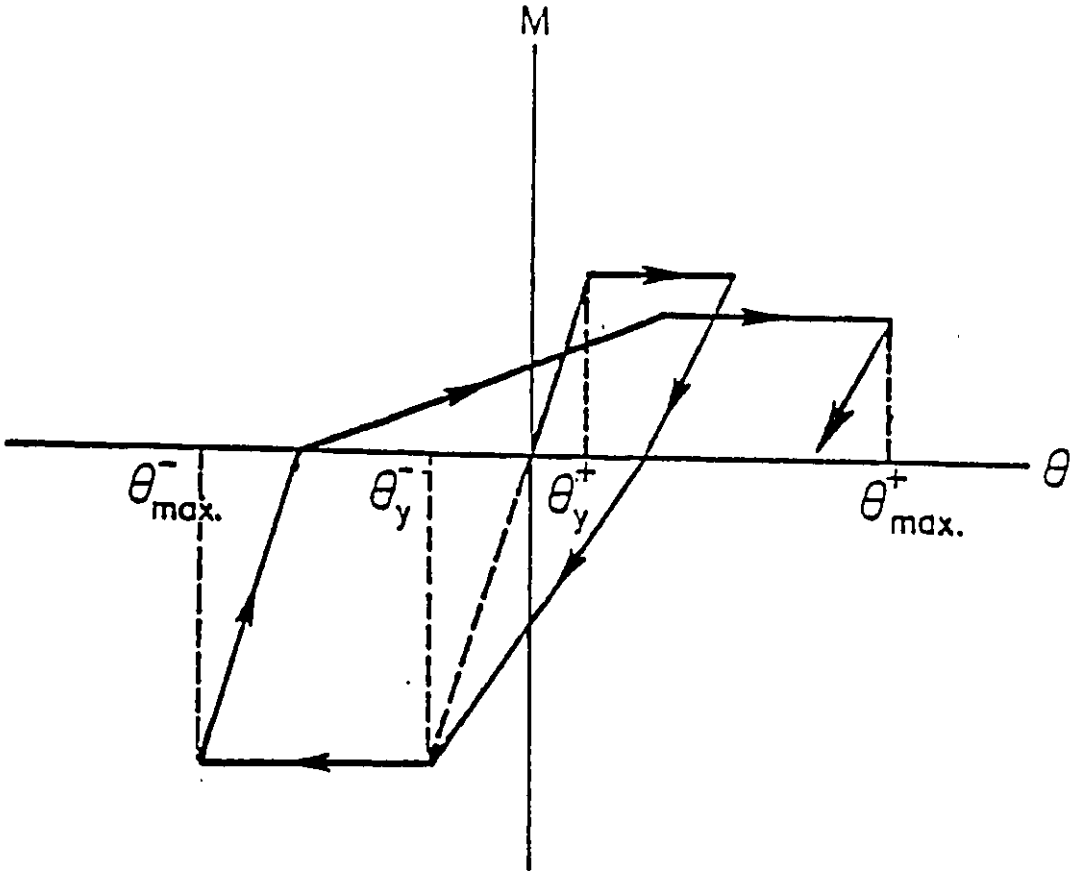

Figure 3.9: Definition of Rotational Ductility Factors

structures may be in order due to the nature of hysteretic loops for this kind of structure. Because of the coupling action between the walls, magnitudes of axial forces at yielding and at the point of maximum rotation may be different. In this investigation, yield rotation corresponding in sign to the maximum rotation is used in defining ductility, irrespective of corresponding axial force levels. Thus, if maximum rotation is positive, rotation at first yield when moment is positive is used to calculate the ductility ratio.

This is illustrated in Fig. 3.9. Another feature of the hysteretic loop for the coupled walls is the loss of symmetry in wall behavior under reversed loading. Thus, axial force in a coupled wall can be tensile when bending in one direction, and compressive when loaded in the opposite direction . Because yield moment of a section changes with magnitude of the concurrent axial force, different values of yield moment and rotation generally result for each direction. In this investigation, the ductility factor is based on the maximum and yield rotations in the same direction. This is done even if the first yield occurs in one direction and maximum rotation is recorded in the opposite direction, although this case rarely occurs. Usually both initial yield and maximum rotation occur while loading in the same direction. Maximum rotation generally occurs during the "tension phase" when the flexural yield level of the wall is reduced due to tension.

Chapter 4

Results of Dynamic Analysis

4.1 General

A total of 20 coupled wall structures were analyzed in this investigation. The three structures selected and discussed in Chapter 2 formed the basis for overall geometric properties of structures. Each of these three structures had a different building height but otherwise had the same overall geometry, fundamental period and beam-to-wall stiffness ratio. Each structure was analyzed with different levels of yield strength and two different levels of beam-to-wall strength ratio. This resulted in a total of 20 cases. Table 4.1, together with table 2.1 provide summary of structural and ground motion parameters used in each case. The results are presented in the form of rotational ductility ratios along building height. Both coupling beam and

structural wall ductilities are illustrated. The results were analyzed to show variation of ductility requirements in members with building height.

4.2 Analysis of 10-Storey Structures

Dynamic inelastic analyses of six 10 storey structures, with initial fundamental period of 1.5 sec, were carried out. Ground motion and structural properties of members are listed in Tables 2.1. and 4.1.

Two different sets of structures were analyzed. The first set included structures with the same beam-to-wall stiffness, and strength ratios, but different beam and wall strengths. The results are shown in Figs. 4.1 and 4.2 in the form of rotational ductility ratios. It is evident in these figures that the ductility requirements decrease with increasing strength. The ductility requirement is high at the wall base, and in the beams of fifth to seventh floors.

To investigate the significance of beam-to-wall strength ratio, three additional analyses were conducted in the second set, using a higher beam-to-wall strength ratio. Response envelopes are shown in Figs. 4.3 and 4.4. This set included structures with strong coupling beams. Therefore the beam ductility requirements were lower than those indicated by the previous set of analyses.

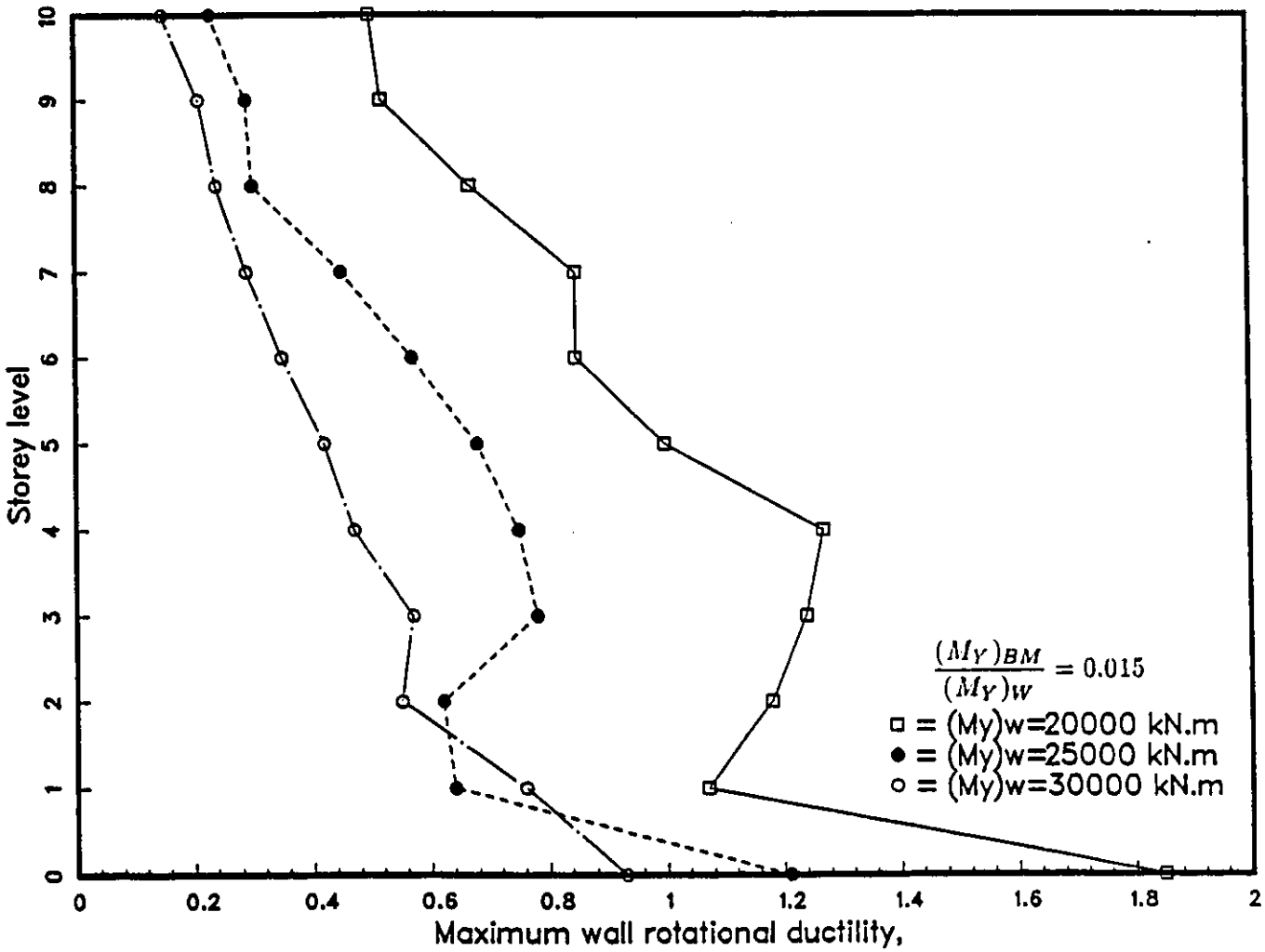

Figure 4.1: Variation of Wall Ductility Demands Along Structure Height -10 Storey Structure

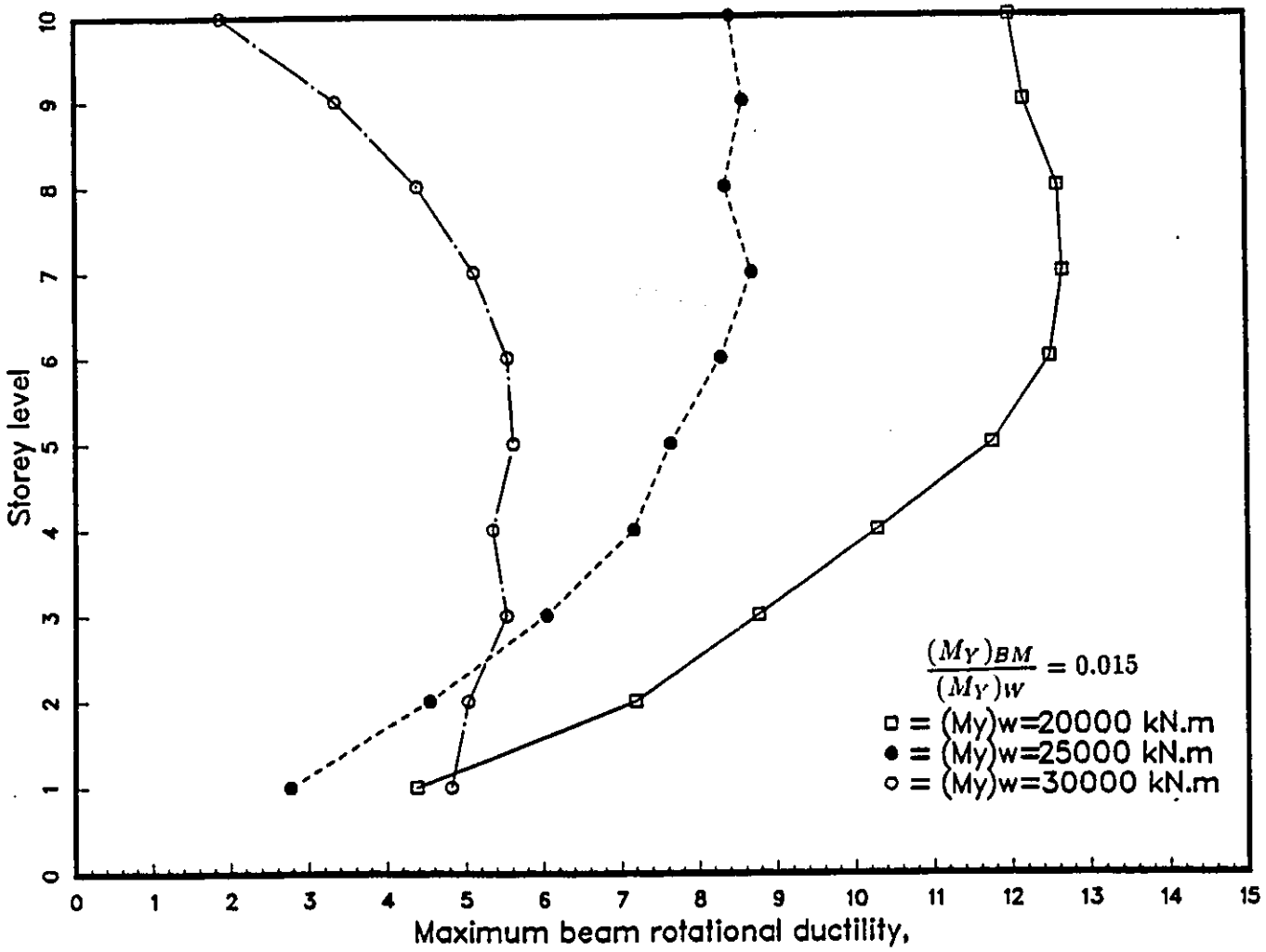

Figure 4.2: Variation of Beam Ductility Demands Along Structure Height - 10 Storey Structure

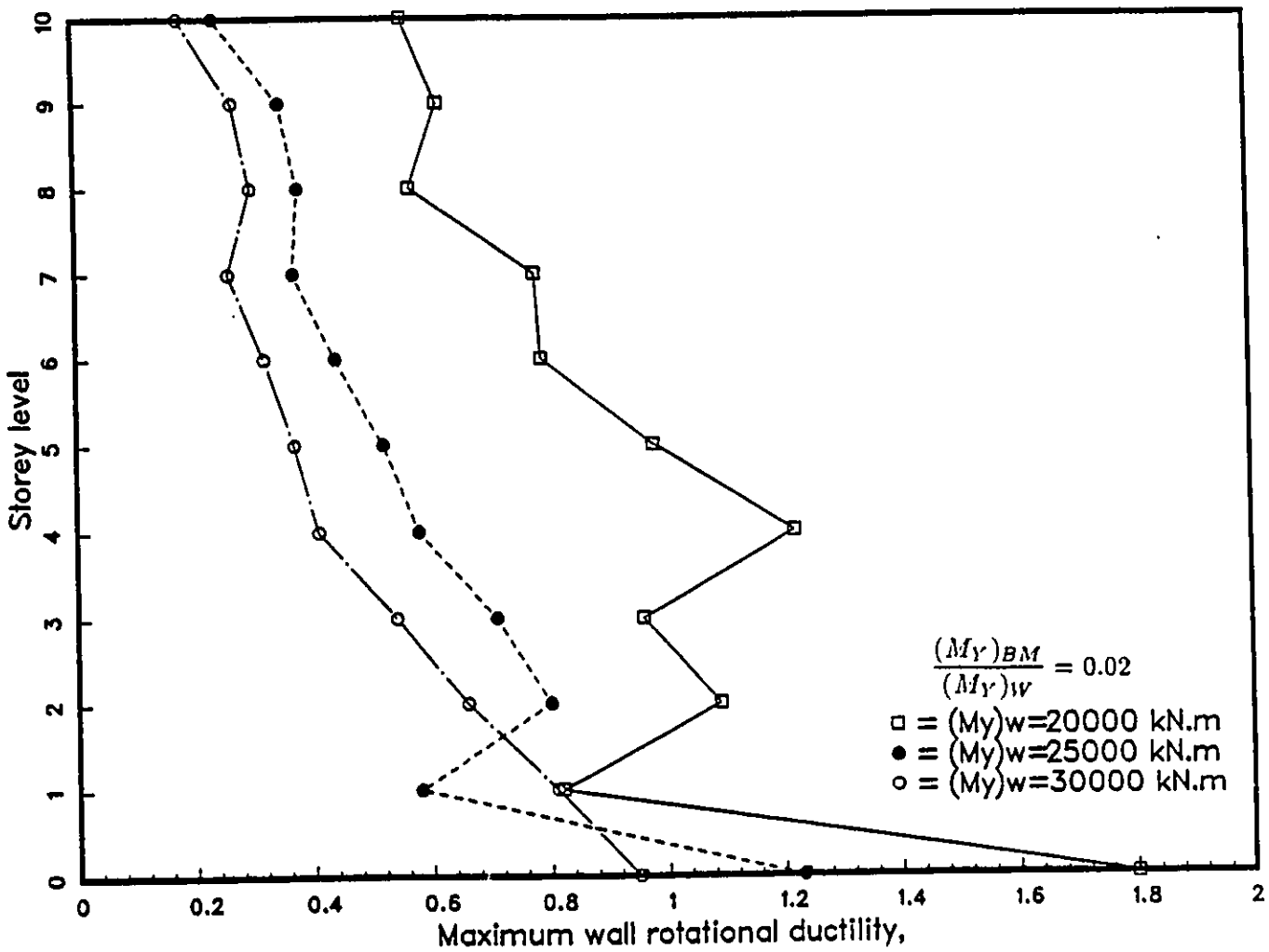

Figure 4.3: Variation of Wall Ductility Demands Along Structure Height - 10 Storey Structure

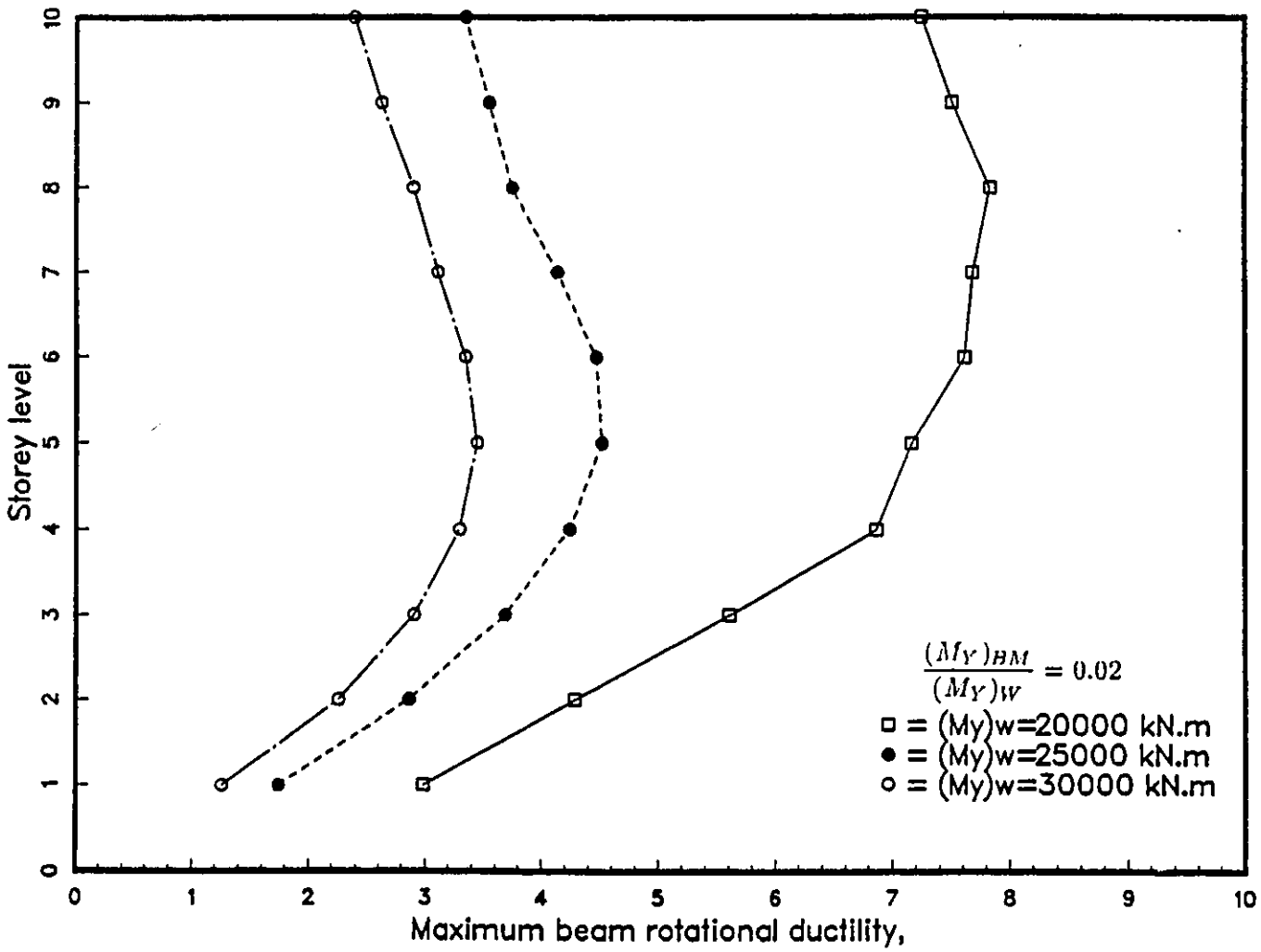

Figure 4.4: Variation of Beam Ductility Demands Along Structure Height - 10 Storey Structure

4.3 Analysis of 20-Storey Structures

Dynamic inelastic analyses of eight 20-storey structures, with initial fundamental period of 1.5 sec, were carried out. Ground motion and structural properties of members are listed in Tables 2.1. and 4.1. Two different sets of structures were analyzed. The first set included structures with the same beam-to-wall stiffness and strength ratios and different beam and wall strengths. The results are shown in Figs. 4.5 and 4.6 in the form of rotational ductility ratios. It is evident in these figures that the ductility requirements decrease with increasing strength. The ductility requirement is high at the wall base and in the beams of seventh to twelveth floors.

To investigate the significance of beam-to-wall strength ratio, three additional analyses were conducted in the second set, using a higher beam-to-wall strength ratio. Response envelopes are shown in Figs.4.7 and 4.8. This set included structures with strong coupling beams. Therefore the beam ductility requirements were lower than those indicated by the previous set of analyses.

4.4 Analysis of 30-Storey Structures

Dynamic inelastic analyses of six 30-storey structures, with initial fundamental period of 1.5 sec, were carried out. Ground motion and structural properties of members are listed in Tables 2.1. and 4.1. Two diffferent

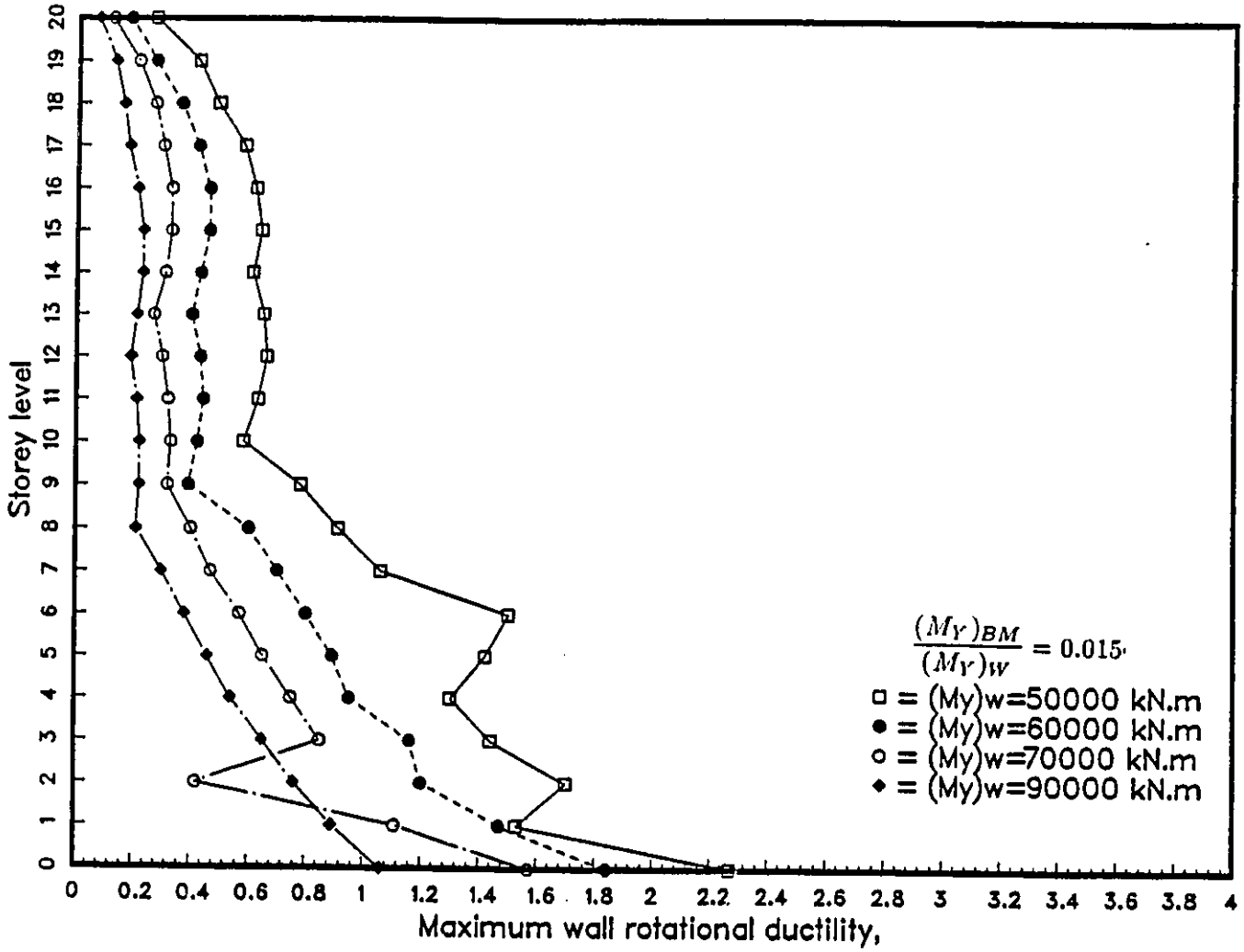

Figure 4.5: Variation of Wall Ductility Demands Along Structure Height - 20 Storey Structure

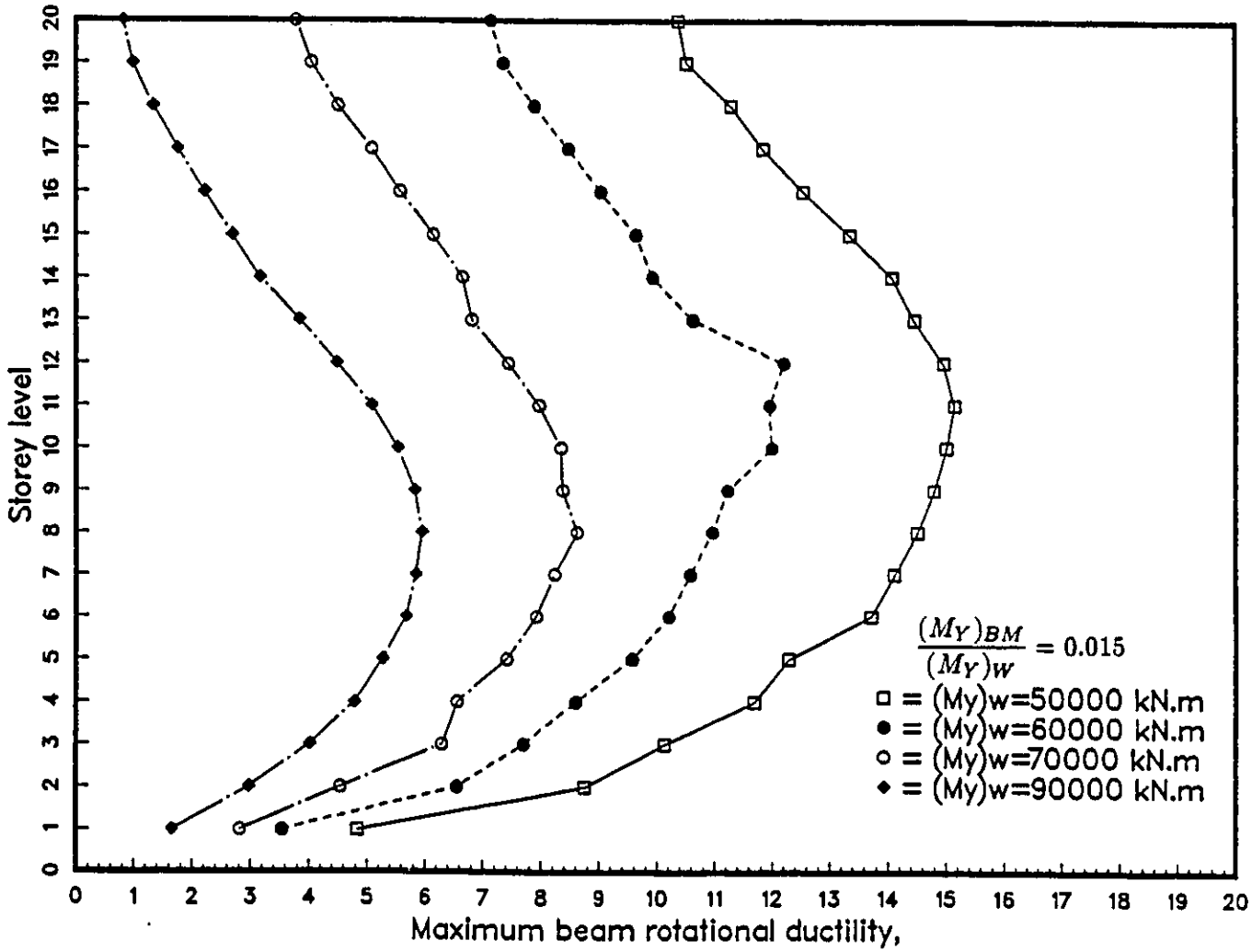

Figure 4.6: Variation of Beam Ductility Demands Along Structure Height - 20 Storey Structure

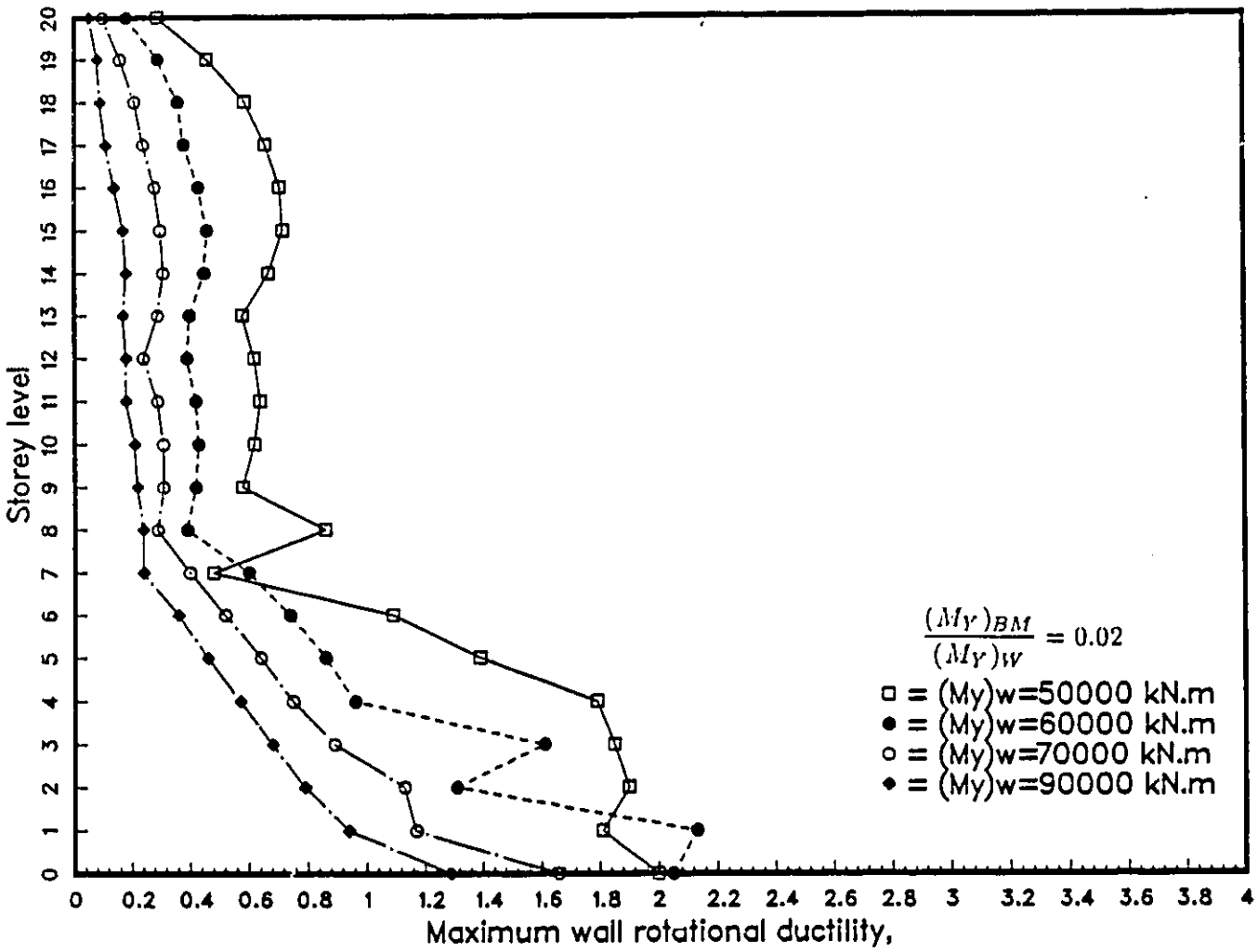

Figure 4.7: Variation of Wall Ductility Demands Along Structure Height - 20 Storey Structure

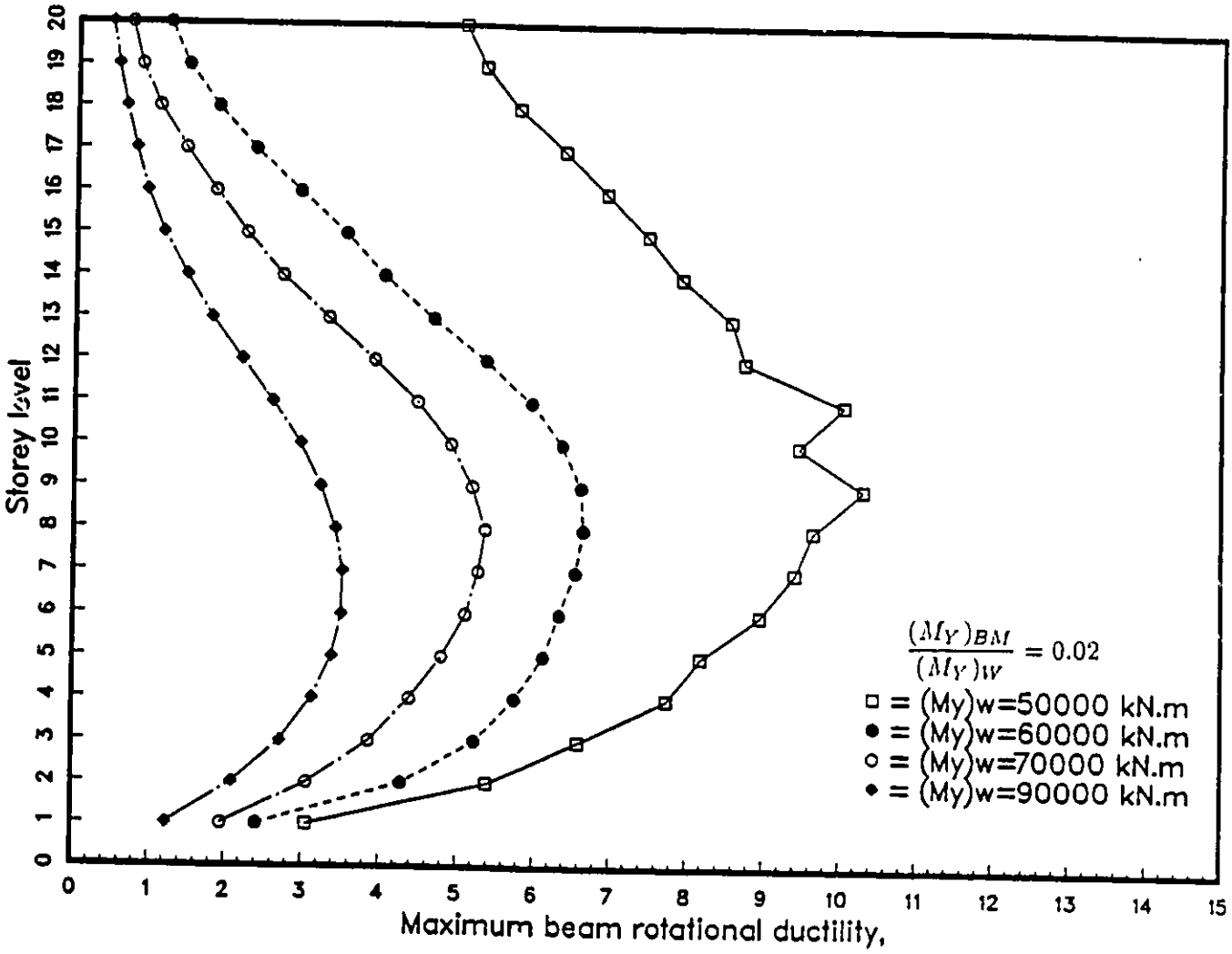

Figure 4.8: Variation of Beam Ductility Demands Along Structure Height - 20 Storey Structure

sets of structures were analyzed. The first set included structures with the same beam-to-wall stiffness and strength ratios, but different beam and wall strengths. The results are shown in Figs. 4.9 and 4.10 in the form of rotational ductility ratios. It is evident in these figures that the ductility requirements decrease with increasing strength. The ductility requirement is high at the wall base, and beams of eight to tenth floors.

To investigate the significance of beam-to-wall strength ratio, three additional analyses were conducted in the second set, using a higher beam-to-wall strength ratio. Response envelopes are shown in Figs. 4.11 and 4.12. This set included structures with strong coupling beams. Therefore the beam ductility requirements were lower than those indicated by the previous set of analyses.

4.5 Effect of Structure Height on Ductility Requirements

The analyses results were examined to investigate the effect of structure height on ductility requirements. It was clear that taller buildings would be more critical in flexure and hence would require higher member strength. During the analysis, it was found essential to increase strength in taller structures to arrive at similar ductility requirements as those for shorter structures. However, presently the relationship between strength increase

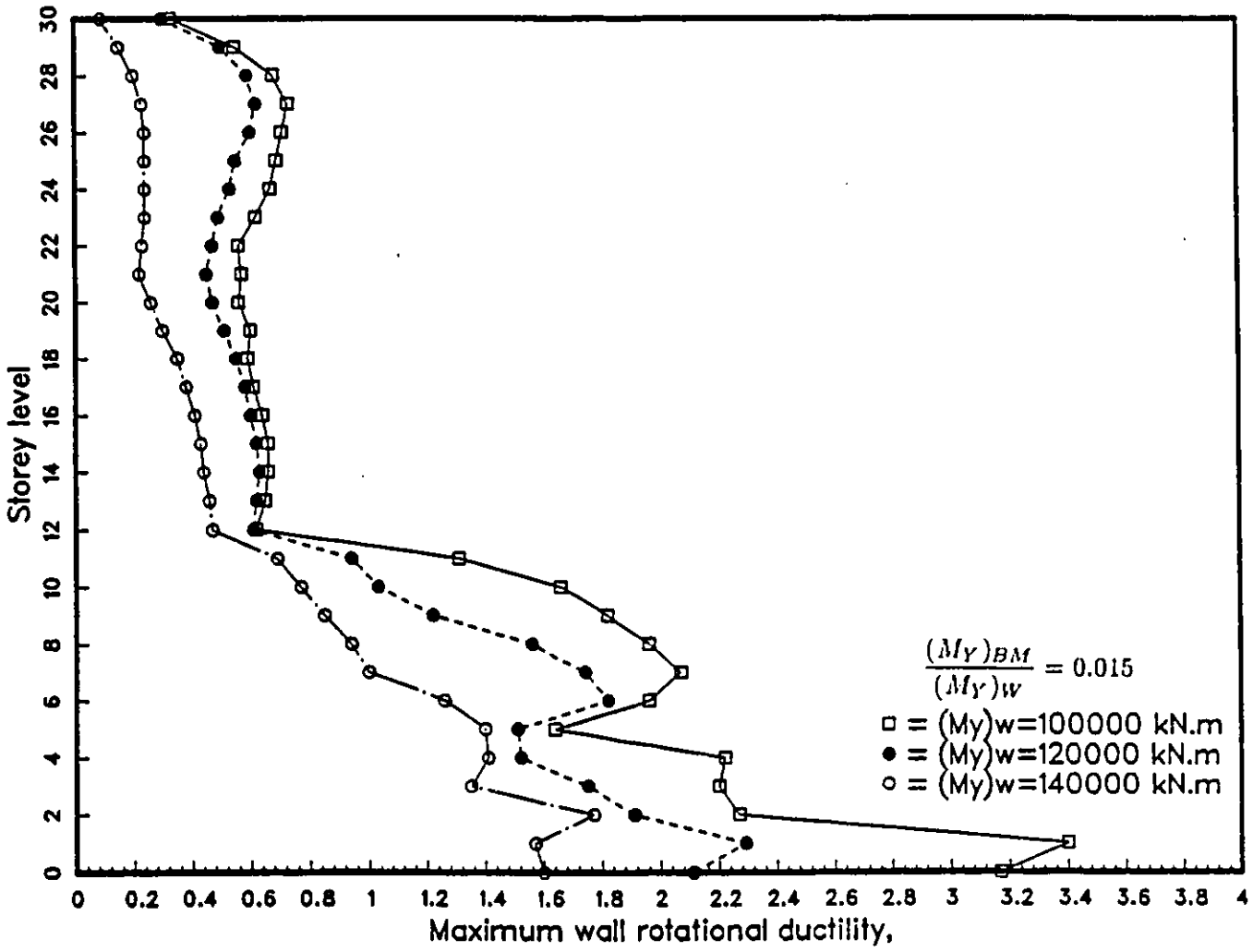

Figure 4.9: Variation of Wall Ductility Demands Along Structure Height - 30 Storey Structure

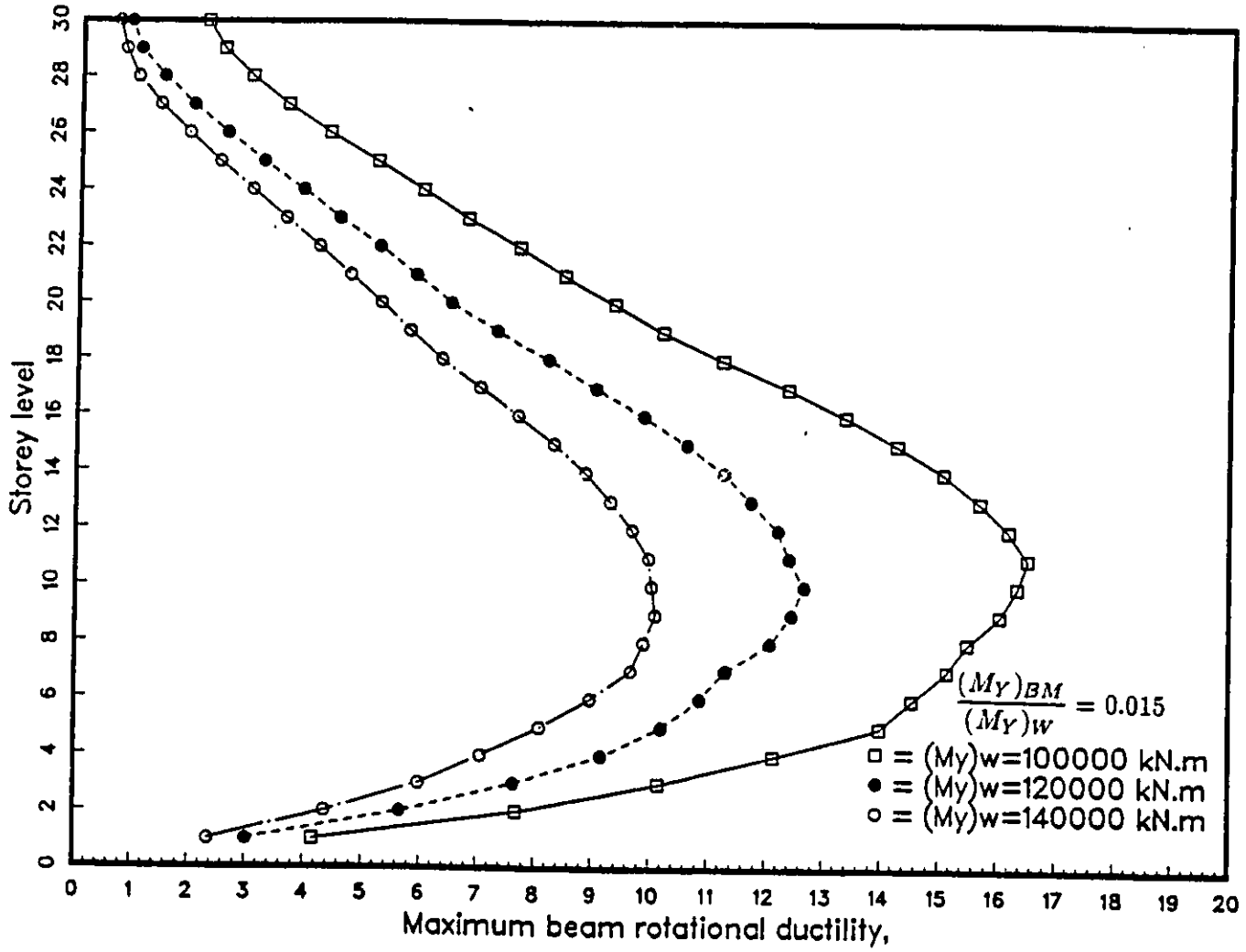

Figure 4.10: Variation of Beam Ductility Demands Along Structure Height - 30 Storey Structure

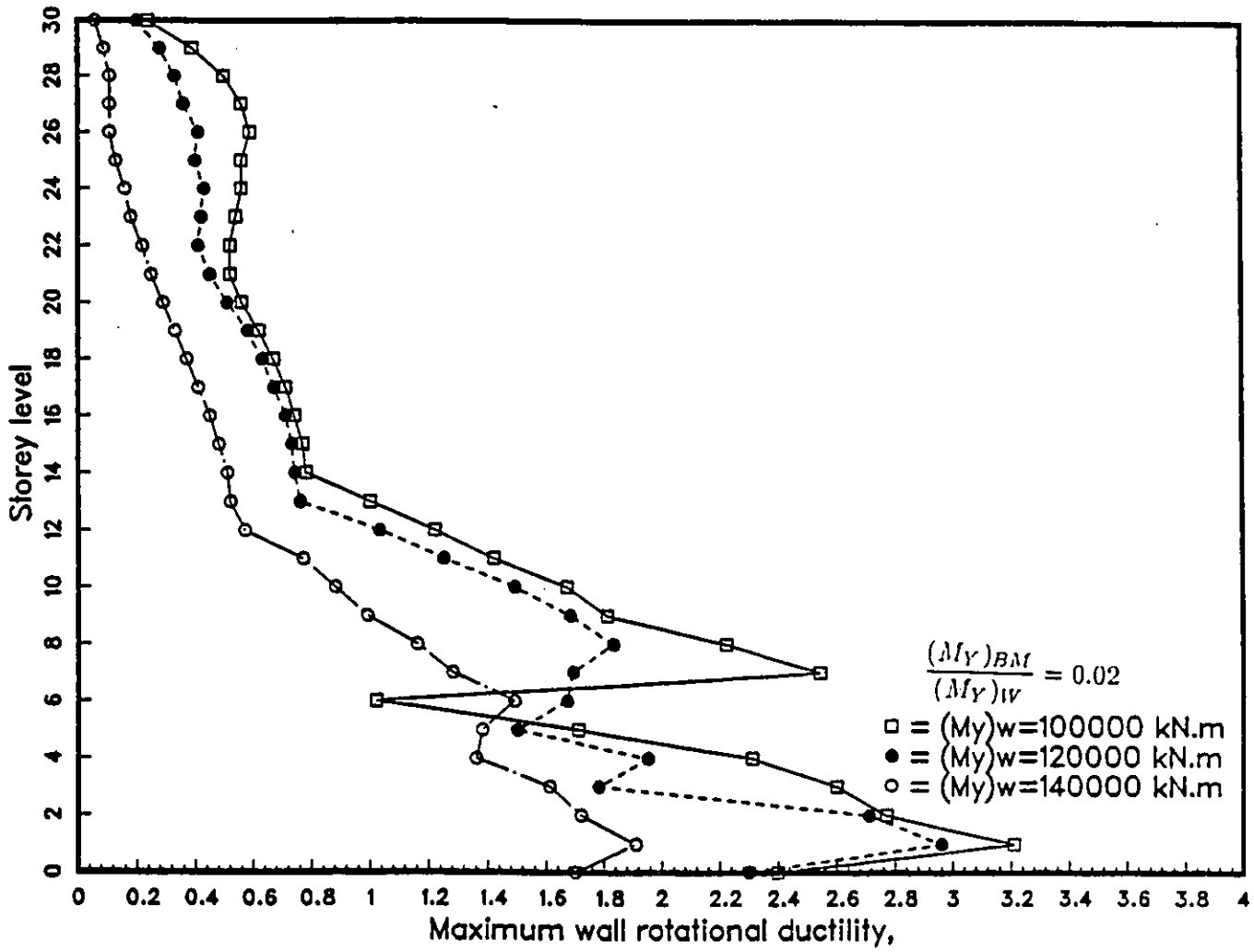

Figure 4.11: Variation of Wall Ductility Demands Along Structure Height - 30 Storey Structure

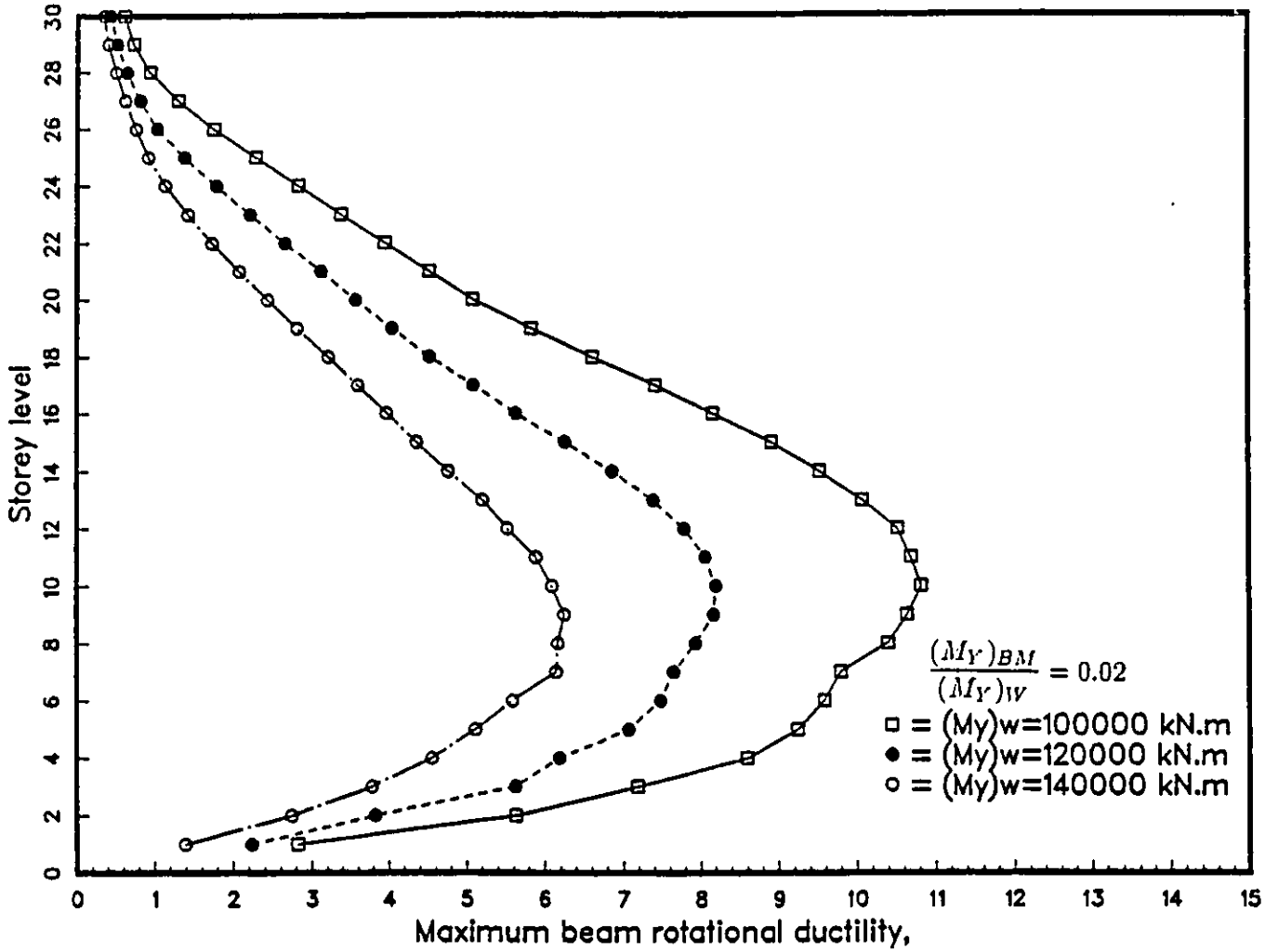

Figure 4.12: Variation of Beam Ductility Demands Along Structure Height - 30 Storey Structure

required in a structure of specific height and required ductility levels is not known. The main objective of the current study is to establish the relationship between height, strength and ductility requirement.

Examination of the analyses results indicates that if wall strength is normalized by the number of stories, ductility requirements vary approximately linearly with the number of stories. Tables 4.2 and 4.3 contain wall yield strengths, normalized strengths and corresponding maximum wall and beam ductility ratios. The ductility ratios in these tables were obtained from dynamic inelastic analyses. Some of the values were obtained by interpolation.

The maximum wall and beam ductility requirements are plotted against number of stories for different strength levels, in Figs. 4.13 to 4.16. The figures indicate that ductility requirements are more sensitive to building height in the high inelasticity range. As maximum deformations approach yield deformations, i.e. as the ductility ratios approach 1.0, the effect of building height becomes less noticeable. The ductility requirements vary exponentially with reduction in strength.

An effort was made to express maximum wall and beam ductility requirements analytically for the coupled wall structures considered in this investigation. The dynamic inelastic response analysis results, tabulated in Tables 4.2 and 4.3 were used to fit curves to data points. The following expressions were obtained for the maximum ductility ratios.

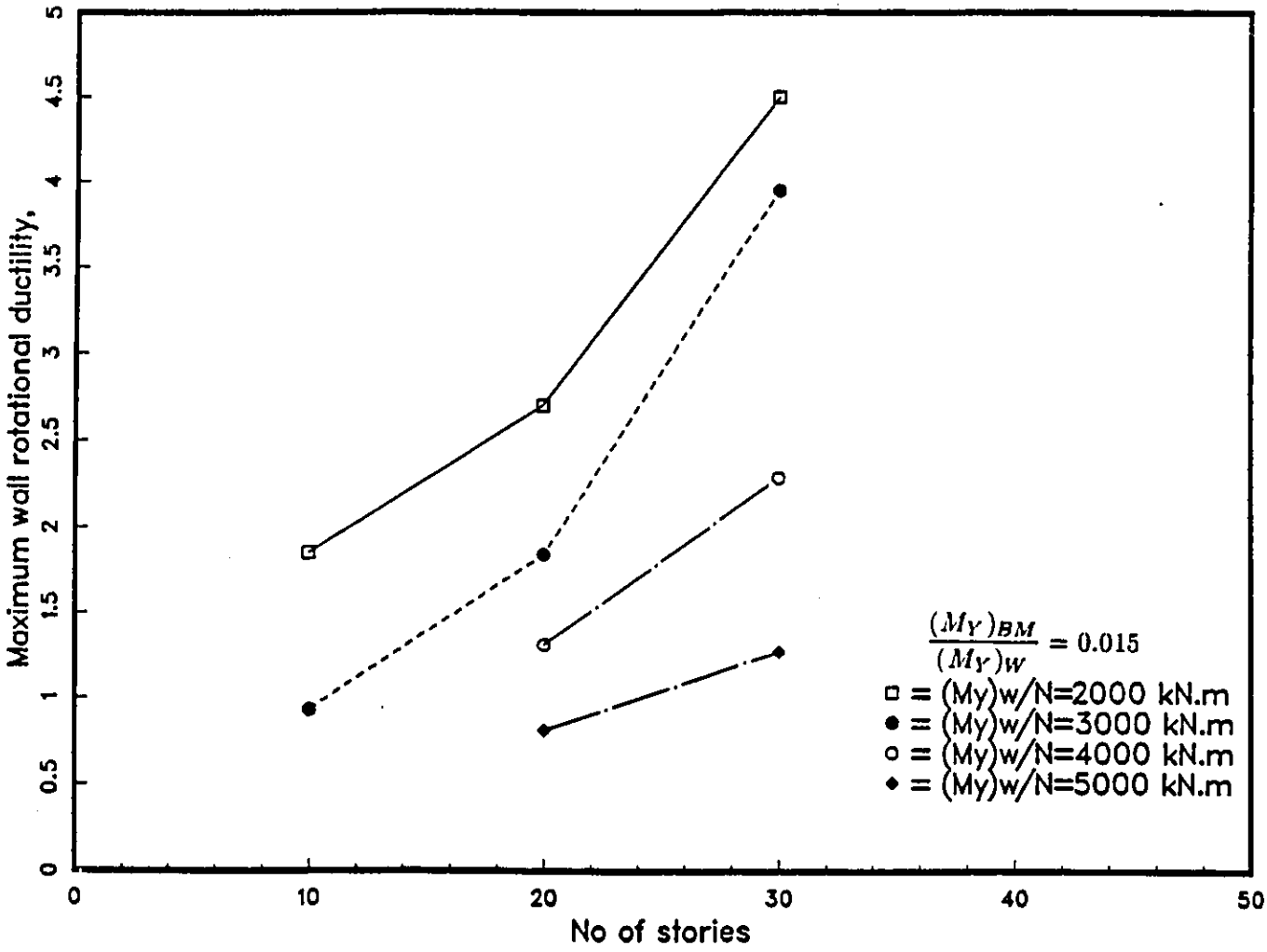

Figure 4.13: Variation of Maximum Wall Ductility Demand with Number of Stories

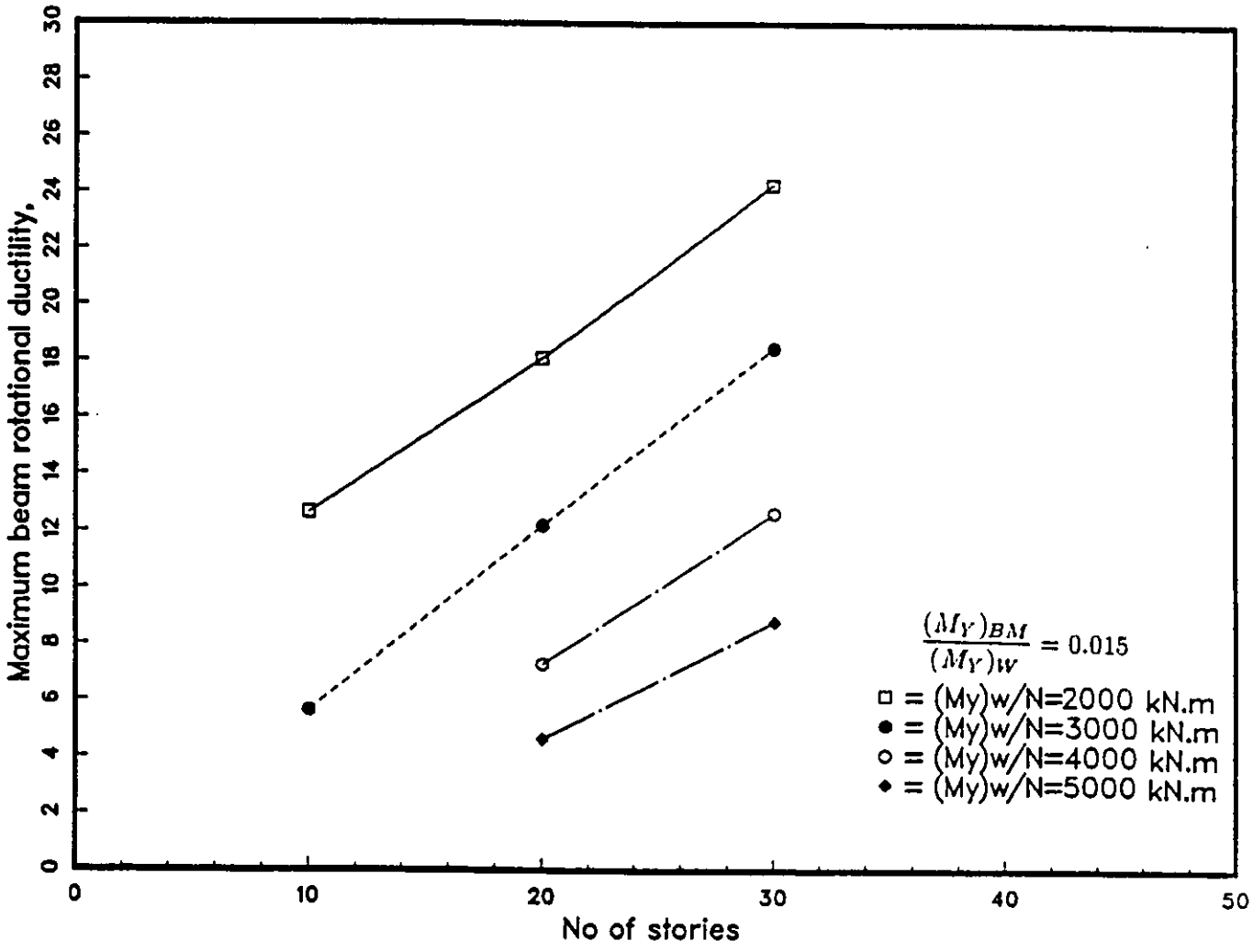

Figure 4.14: Variation of Maximum Beam Ductility Demand with Number of Stories

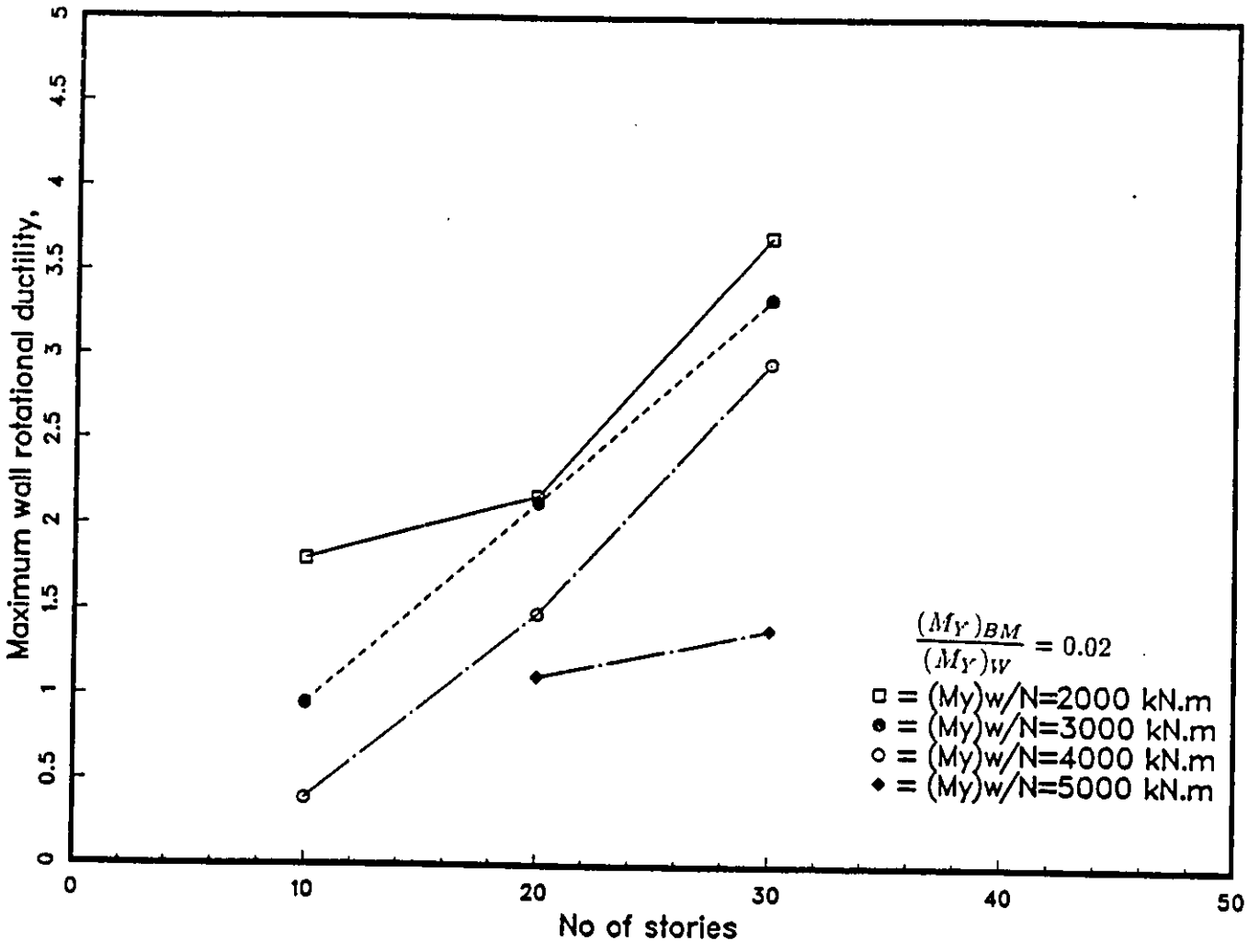

Figure 4.15: Variation of Maximum Wall Ductility Demand with Number of Stories

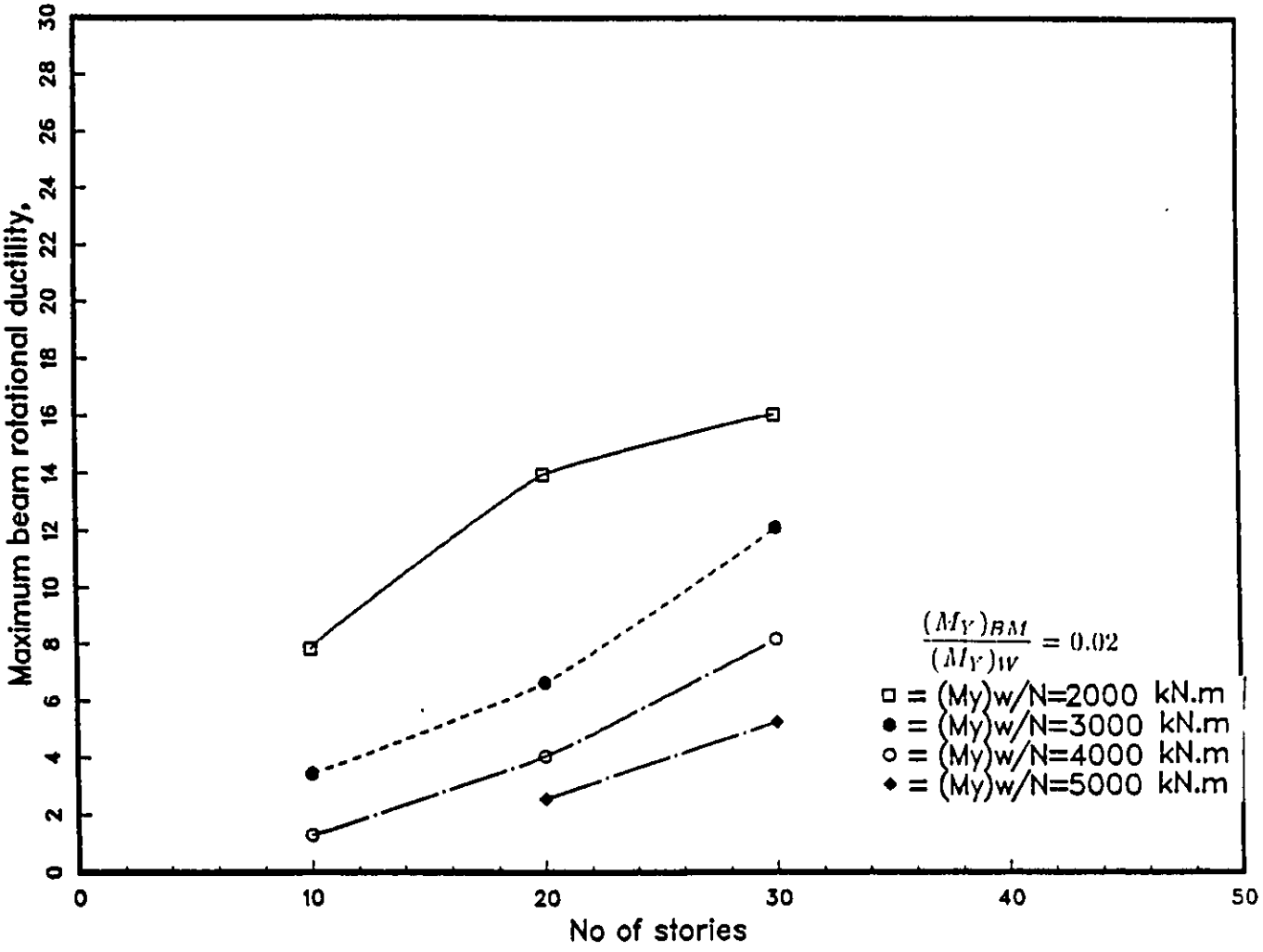

Figure 4.16: Variation of Maximum Beam Ductility Demand with Number of Stories

For coupled walls with beam-to-wall strength ratio of 0.015 :

$$(\mu_{max})_{wall} = 12.3 - 1.6 \ln \frac{(M_Y)_w}{N} + 0.35e^{-3.7\times10^{-4}\frac{(M_Y)_w}{N}}N \qquad (4.1)$$

$$(\mu_{max})_{beam} = 100 - 12.5 \ln \frac{(M_y)_w}{N} + 0.80e^{-1.2\times10^{-4}\frac{(M_y)_w}{N}}N \qquad (4.2)$$

where; $(M_Y)_w$ is in kN.m

For coupled walls with beam-to-wall strength ratio of 0.02 :

$$(\mu_{max})_{wall} = 18.3 - 2.3 \ln \frac{(M_y)_w}{N} + 0.08e^{1.0\times10^{-4}\frac{(M_y)_w}{N}}N \qquad (4.3)$$

$$(\mu_{max})_{beam} = 63.3 - 7.9 \ln \frac{(M_y)_w}{N} + 0.61e^{-1.5\times10^{-4}\frac{(M_y)_w}{N}}N \qquad (4.4)$$

where; $(M_Y)_w$ is in kN.m

Figures 4.17 to 4.20 illustrate the above relationships and their correlations with the results of dynamic inelastic analysis. These expressions are highly empirical in nature and very limited in scope. A more accurate application of this approach would be to estimate maximum ductility ratios for a coupled wall structure when the same is available for the same structure with different building height. One of the main objectives of this research project is to be able to extrapolate analysis results of a specific structure to structures with different building heights, while keeping the other properties constant. This can be done by using the slopes of the above expressions.

The analytical expressions, given in Eqs 4.1 through 4.4 cover two different levels of beam-to-wall strength ratio. The analysis results, as well as previous

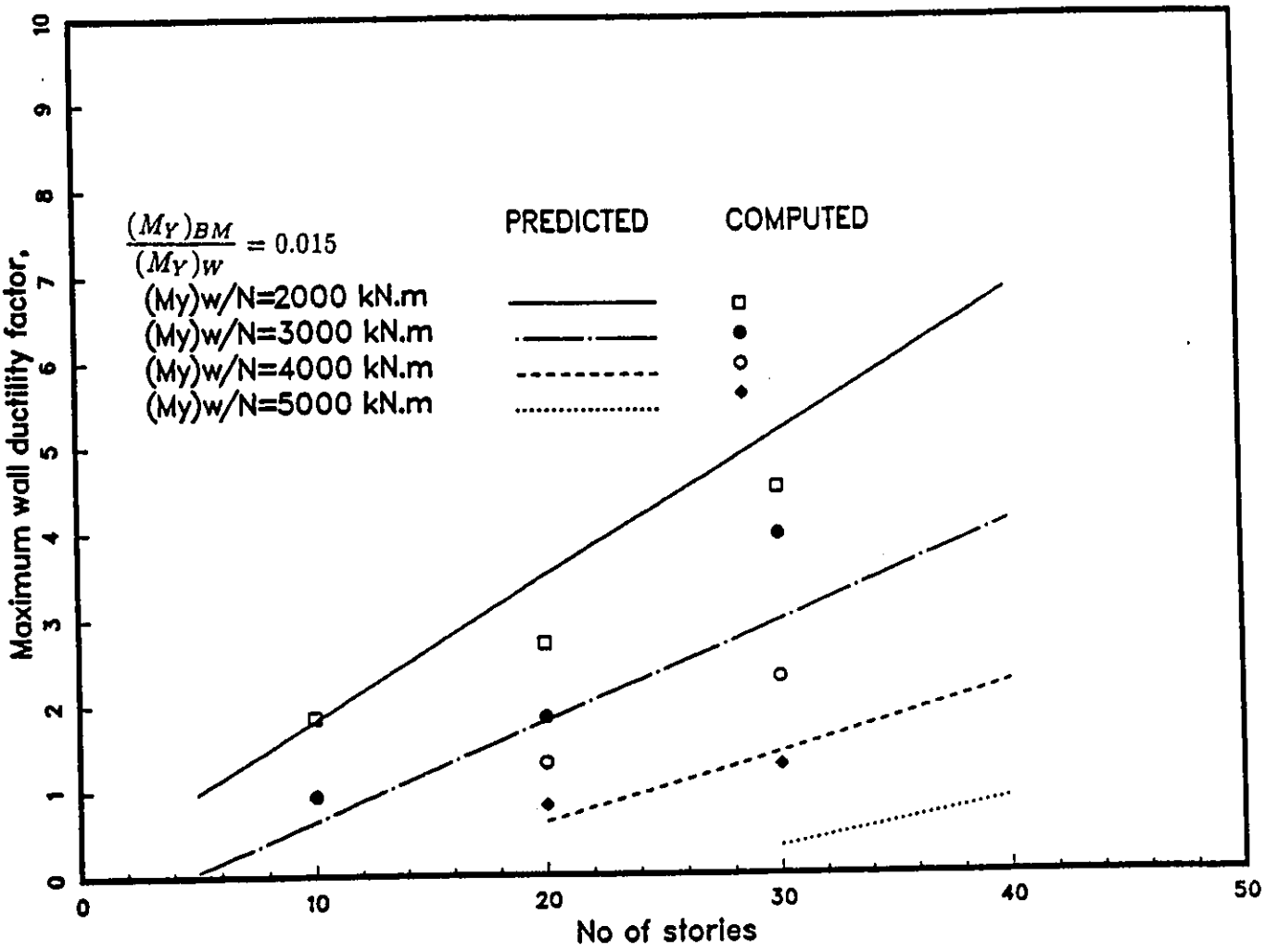

Figure 4.17: Comparison of Predicted and Computed Maximum Wall Ductility Demands

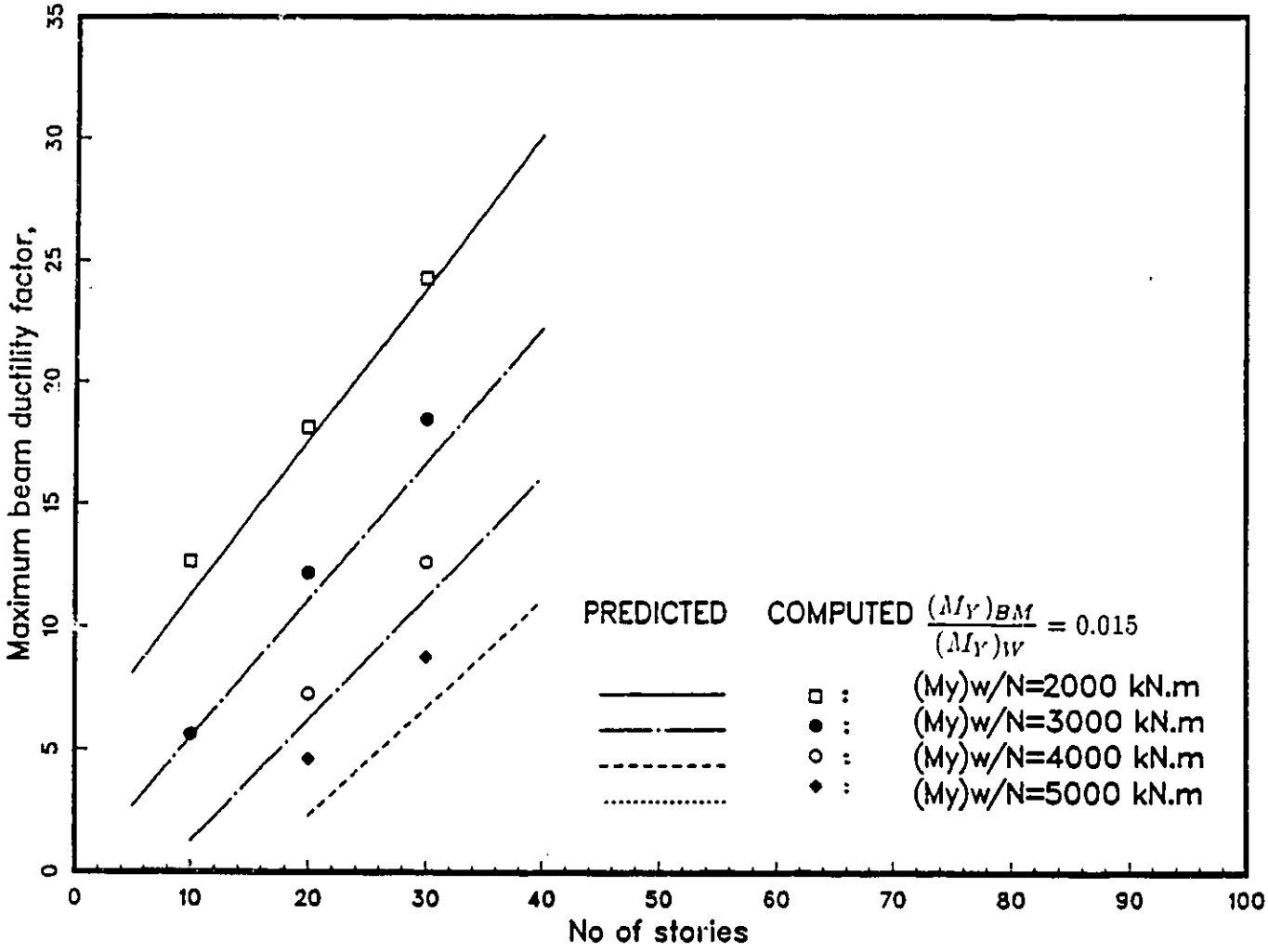

Figure 4.18: Comparison of Predicted and Computed Maximum Beam Ductility Demands

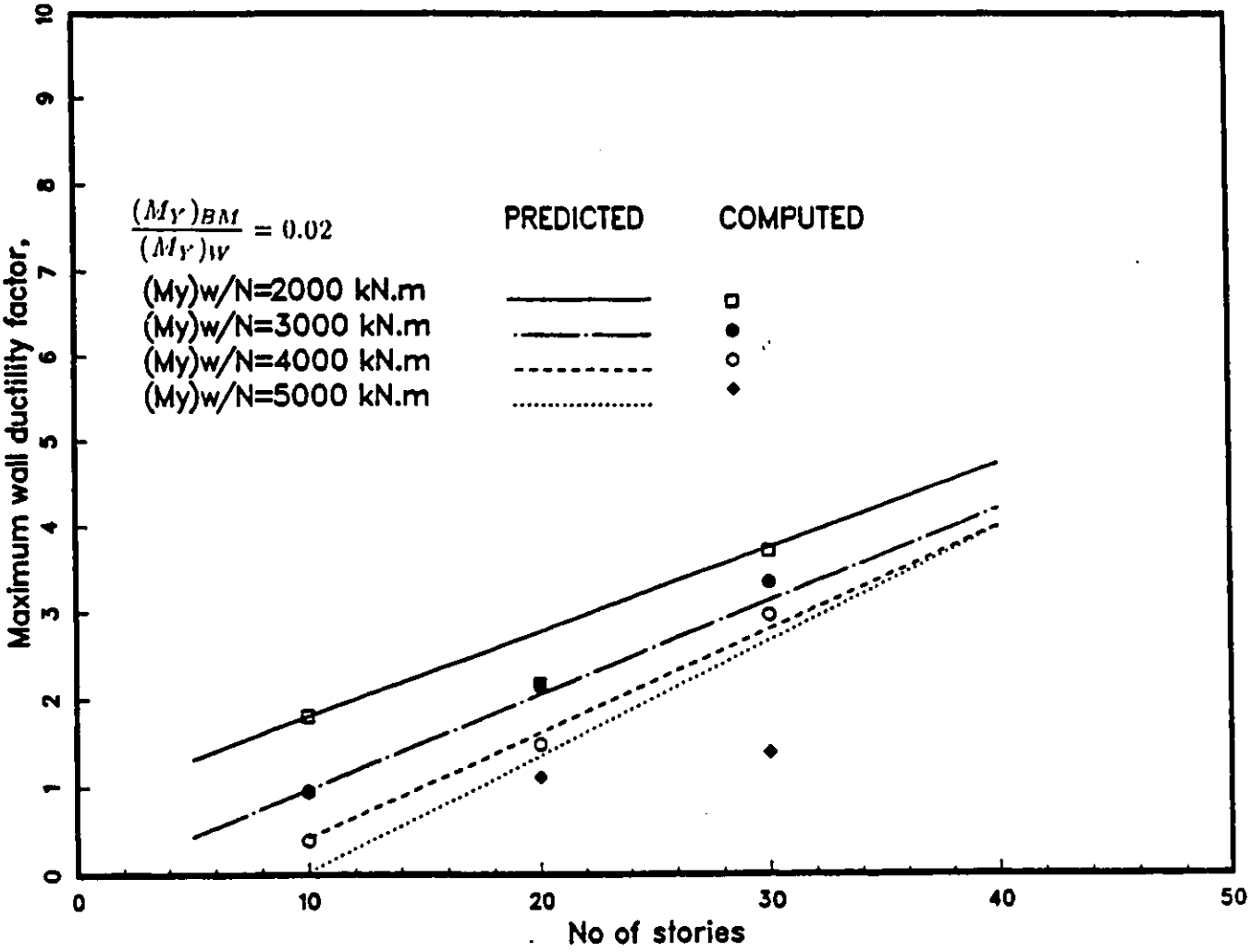

Figure 4.19: Comparison of Predicted and Computed Maximum wall Ductility Demands

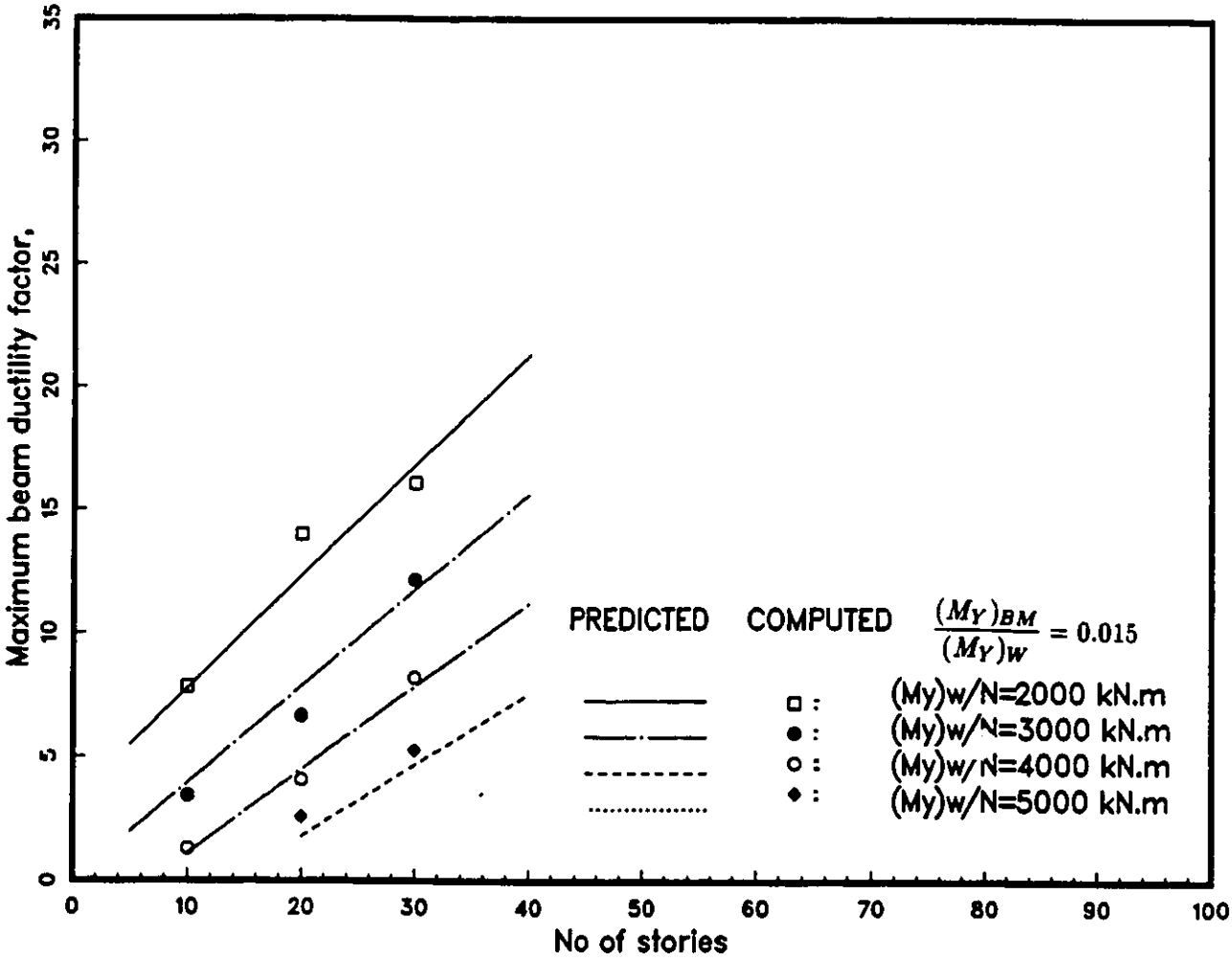

Figure 4.20: Comparison of Predicted and Computed Maximum Beam Ductility Demands

literature (1,2,3.) indicate that beam ductility requirement is sensitive to beam-to-wall strength ratio.

The available data indicates that the slope of the curve that shows the variation of maximum ductility requirement with number of stories varies in proportion to the beam-to-wall strength ratio. The following expression is derived to predict maximum beam ductility requirements in coupled walls with different beam-to-wall strength ratios and building heights if the ductility ratio is known for a given building height.

$$(\mu_2)_{BM} = (\mu_1)_{BM} + \alpha(N_2 - N_1)e^{-1.35\times10^{-4}\beta} \tag{4.5}$$

where;

$\alpha = \frac{0.012}{R}$

R=Beam-to-Wall Strength Ratio

$\beta = \frac{(M_Y)_w}{N}$

N_1 *and* $(\mu_1)_{BM}$ are, the number of stories and maximum beam ductility ratio respectively, for the first building for which this information is known. N_2 *and* $(\mu_2)_{BM}$ are, the number of stories and maximum beam ductility ratio respectively, for the second building for which the ductility ratio is to be determined. The factor β is the ratio of wall flexural strength to number of stories. N is equal to N_1 and N_2 for the first and second structures respectively and the factor β must be constant for both structures for the above expression to be applicable.

The wall ductility requirement is not sensitive to variations in beam-to-wall strength ratio. It was found that the slopes of the relationships that give variation of wall ductilities with number of stories for the two beam-to-wall strength ratios considered, were similar. Therefore the following expression is proposed to predict maximum wall ductility requirement of a building if this information is known for a similar building with different height.

$$(\mu_2)_{wall} = (\mu_1)_{wall} + 0.08(N2 - N1)e^{1.0\times10^{-4}\beta} \tag{4.6}$$

where;

$$\beta = \frac{(M_Y)_w}{N}$$

The symbols used in the above expression are the same as those used previously in Eq (4.5) with the exception of the beam ductility ratios replaced by the wall ductility ratios.

Equations (4.5) and (4.6) provide means of predicting ductility demands of a structure if dynamic inelastic analysis results are available for another structure with different height but the same structural properties otherwise. As an example, if a structural engineer knows the response of a 20-storey coupled wall structure, and associated ductility demands for this structure, and would like to see the consequences of changing the structure height to 25 stories, then the above equations can be used to predict the response. These expressions are especially useful if design data is prepared systematically for one building height and the same is required for another building height.

Table 4.1: Properties of Structures considered in Analyses

Structure Label	No of stories	T (sec)	$\frac{(kEI/l)_{BM}}{(kEI/l)_W}$	$(M_Y)_W$ (kN.m)	$(M_Y)_{BM}$ (kN.m)	$\frac{(M_Y)_{BM}}{(M_Y)_w}$
1001	10	1.5	0.03007	20,000	300	0.015
1002	10	1.5	0.03007	25,000	375	0.015
1003	10	1.5	0.03007	30,000	450	0.015
1004	10	1.5	0.03007	20,000	400	0.020
1005	10	1.5	0.03007	25,000	500	0.020
1006	10	1.5	0.03007	30,000	600	0.020
2001	20	1.5	0.03007	50,000	750	0.015
2002	20	1.5	0.03007	60,000	900	0.015
2003	20	1.5	0.03007	70,000	1050	0.015
2004	20	1.5	0.03007	90,000	1350	0.015
2005	20	1.5	0.03007	50,000	1000	0.020
2006	20	1.5	0.03007	60,000	1200	0.020
2007	20	1.5	0.03007	70,000	1400	0.020
2008	20	1.5	0.03007	90,000	1800	0.020
3001	30	1.5	0.03007	100,000	1500	0.015
3002	30	1.5	0.03007	120,000	1800	0.015
3003	30	1.5	0.03007	140,000	2100	0.015
3004	30	1.5	0.03007	100,000	2000	0.020
3005	30	1.5	0.03007	120,000	2400	0.020
3006	30	1.5	0.03007	140,000	2800	0.020

Table 4.2: Maximum Wall and Beam Ductilities

Structure Label	No. of stories	$(M_Y)_w$ (kN.m)	$\frac{(M_Y)_{BM}}{(M_Y)_W}$	$\frac{(M_Y)_w}{N}$	$(\mu_w)_{max}$	$(\mu_{BM})_{max}$
1001	10	20,000	0.015	2000	1.85	12.66
1002	10	25,000	0.015	2500	1.21	8.69
1003	10	30,000	0.015	3000	0.93	5.63
2010[1]	20	40,000	0.015	2000	2.70	18.10
2001	20	50,000	0.015	2500	2.27	15.15
2002	20	60,000	0.015	3000	1.84	12.20
2003	20	70,000	0.015	3500	1.57	8.61
2009[1]	20	80,000	0.015	4000	1.31	7.28
2004	20	90,000	0.015	4500	1.06	5.94
2011[1]	20	100,000	0.015	5000	0.81	4.61
3007[1]	30	60000	0.015	2000	4.50	24.3
3008[1]	30	90000	0.015	3000	3.95	18.47
3001	30	100000	0.015	3333	3.40	16.53
3002	30	120,000	0.015	4000	2.29	12.65
3003	30	140,000	0.015	4667	1.60	10.08
3009[1]	30	150,000	0.015	5000	1.26	8.80

[1]These cases were obtained through interpolation or exterpolation of existing data.

Table 4.3: Maximum Wall and Beam Ductilities

Structure Label	No. of stories	$(M_Y)_w$ (kN.m)	$\frac{(M_Y)_{BM}}{(M_Y)_W}$	$\frac{(M_Y)_w}{N}$	$(\mu_w)_{max}$	$(\mu_{BM})_{max}$
1004	10	20,000	0.02	2000	1.80	7.83
1005	10	25,000	0.02	2500	1.23	4.51
1006	10	30,000	0.02	3000	0.95	3.44
1007[1]	10	40,000	0.02	4000	0.39	1.3
2011[1]	20	40,000	0.02	2000	2.17	13.96
2005	20	50,000	0.02	2500	2.00	10.30
2006	20	60,000	0.02	3000	2.13	6.64
2007	20	70,000	0.02	3500	1.66	5.35
2012[1]	20	80,000	0.02	4000	1.48	4.06
2008	20	90,000	0.02	4500	1.29	3.50
2013[1]	20	100,000	0.02	5000	1.11	2.57
3010[1]	30	60000	0.02	2000	3.71	16.07
3011[1]	30	90000	0.02	3000	3.34	12.13
3004	30	100000	0.02	3333	3.21	10.82
3005	30	120,000	0.02	4000	2.96	8.19
3006	30	140,000	0.02	4667	1.91	6.24
3012[1]	30	150,000	0.02	5000	1.39	5.27

[1]These cases were obtained through interpolation or exterpolation of existing data.

Chapter 5

Conclusion

The following conclusions can be made on the basis of the research work reported in this thesis:

1. Ductility demand in coupled wall structures increases with increasing building height. Maximum wall and beam ductility demands increase exponentially with an increase in building height.

2. The relationship between rotational ductility ratio and number of stories is approximately linear when wall strength is adjusted in proportion to the number of stories. This relationship is based on constant fundamental period, beam-to-wall strength and stiffness ratio, and ground motion parameters.

3. The effect of building height on rotational ductility demand is low when limited inelasticity is observed under earthquake excitation. This effect increases sharply when the observed inelasticity is extensive.

4. In the range considered in this investigation, beam-to-wall strength ratio has a pronounced effect on beam ductilities. Wall ductilities are not affected appreciably by the same parameter.

5. Maximum wall ductility demand occurs at the wall base. Maximum beam ductility demand generally occurs at a storey level corresponding to approximately one third the structure height from the base. As the structure strength decreases and hence the ductility demand increases, this location gradually shifts towards the mid-height.

6. Equations (4.5) and (4.6), developed in this thesis can be used to predict rotational ductility demands of a structure if this information is available for another structure with different height but the same structural and ground motion parameters.

Bibliography

[1] Saatcioglu, M., Corley, W.G., and Derecho, A.T, *Parametric Study of Earthquake-Resistant Coupled Walls,* Journal of Structural Engineering, vol.113, No. 1, January, 1987.

[2] Saatcioglu, M., and Derecho, A.T., *Dynamic inelastic Responce of Coupled Walls as affected by Axial Forces,* Proceeding of the $CSCE-ASCE-ACI-CEB$ International Symposium on "Nonlinear Design of Concrete Structures", SM Study No. 14 , University of Waterloo Press, Waterloo, Ontario, 1980.

[3] Saatcioglu, M., Derecho, A.T., and Corley, W.G., *Modeling Hysteresis Behaviour of Coupled Walls for Dynamic Analysis,* Earthquake Engineering and Structural Dynamics Journal, vol. 11, 1983, pp. 711-726.

[4] Oesterle, R.G., Fiorato, A.E., Aristizabal-Ochoa, J.D., and Corley, W.G., *Hysteresis Responce of Reinforced Concrete Structural Walls,* Publication SP-63, American Concrete Institute, 1980.

[5] Fiorato, A.E., Oesterle, R.G., and Carpenter, J.E., *Reversing Load*

*Tests of Five Isolated Structural Walls,*International symposium on Earthquake Structural engineering, St.Louis, Missouri, USA, August, 1976.

[6] Vitalmo, V.B., *Seismic Behaviour of R/C Wall Structural Systems,* Proceedings of the seventh World Conference on Earthquake engineering, September 1980, Istanbul, Turkey.

[7] Clough, R.W., *Dynamic Effect of Earthquakes,* Proceedings, ASCE, Vol. 86, No. ST4, April 1960

[8] Fintel, M., *Handbook of Concrete Engineering,* Van Nostrand Reinhold Co., Newyork, 1985.

[9] Park, R. and Paulay, T. *Reinforced Concrete Structures,* John Wiley and Sons, inc., 1975.

[10] Takeda, T., Sozen, M.A., and Nielsen, N.N., *Reinforced Concrete Response to Simulated Earthquakes,* Journal of the Structural Division, ASCE, Vol. 96, No. ST-12, Dec. 1970, pp. 2557-2573.

[11] Kanaan, A.E. and Powell, G.H, *General purpose Computer Program for Inelastic Dynamic Response Structures,* Report No. EERC 73-6, Earthquake Engineering Research Center, University of California, Berkeley, April 1973.

[12] Bogdanoff, J.L., *Comments on Seismic Accelerograms and Response Spectra,* (Preliminary Report), Joint U.S.-Japanese Seminar in Applied Stochstics, NSF-JSPS, Tokyo, May 1966.

[13] Saatcioglu, M., Derecho, A.T., Corley W.G., Parmelee, R.A. and Scanlon, A., *Coupled Walls in Earthquake-Resistant Buildings, Prametric Investigation and Design Proceedure* Report to National Science Foundation, Portland Cement Association, july 1981.